UNIVERSITA' DEGLI STUDI DELLA TUSCIA DI VITERBO

Dipartimento di Scienze Ecologiche e Biologiche

CORSO DI DOTTORATO DI RICERCA IN
GENETICA E BIOLOGIA CELLULARE

XXVI Ciclo

Genetic and cytological analysis of two male sterile mutant strains of *Drosophila melanogaster*

BIO/18

Tesi di dottorato di:
Fabiana Fabbretti

Coordinatore del corso
Prof. Giorgio Prantera

Tutore
Prof. Giorgio Prantera

INDEX

ABSTRACT

Spermatogenesis, the production of male functional gametes from germinal stem cells, represents one of the most dramatic examples of cell differentiation. The availability of *Drosophila melanogaster* mutants defective for specific spermatogenesis stages, the short *Drosophila* life cycle, the availability of genetic resources, like a fully sequenced genome, and the gene and pathway conservation with humans, make this insect particularly suitable to study the genetic control of the spermatogenesis process. The aim of my PhD research project was the analysis of two mutant strains (*ms(2)Z5584* and *ms(2)Z1168*) belonging to a unique collection of 13 ethyl-methansulfonate (EMS)-induced male sterile recessive mutants identified in a large screening for male-sterile mutations on chromosome 2 and 3 (Wakimoto et al., 2004). From a preliminary cytological screen of mutations, a general and common aberrant phenotype affecting the entry into and progression of the meiotic cell cycle was identified: mutants skipped one or both meiotic divisions but carried out the differentiation of spermatids although with anomalies.

The *ms(2)Z5584* mutant strain was previously genetically and cytologically characterized and a point mutation in *rae1* gene was identified as responsible of the aberrant phenotypes (Volpi et al., 2013). Starting from that evidences, I confirmed the identification of *rae1* as the gene underlying the *ms(2)Z5584* mutant phenotype, by RNAi silencing of the wild type *rae1*. Then, I uncovered the localization pattern of RAE1 during meiotic cell cycle by GAL4/UAS system allowing the expression of *UASGFP-rae1* transgene under both testis-specific and constitutive drivers. Finally, I performed the phenotype rescue of the *ms(2)Z5584* mutant by using of *UASGFP-rae1* transgene.

The *ms(2)Z1168* mutant strain was cytologically characterized by immunohistochemistry technique using antibodies against several structures involved in male meiosis and confocal microscopy. The *ms(2)Z1168* mutant exhibited anomalies in nuclear lamina structure together with chromatin condensation defects. The *ms(2)Z1168* genetic analysis narrowed the gene locus to a genomic region containing 12 genes. The gene identification was further refined by reverse genetic approach using RNA interference and by sequencing. Mutations affecting a regulatory region of *CG7810* gene were identified in the mutant genome. Finally, since the *ms(2)Z1168* mutant

exhibited nuclear lamina defects, an accurate nuclear lamina characterization during wild type meiosis and spermatogenesis was performed.

The study of mutant strains disrupted for some aspects of spermatogenesis process allows a broader understanding of the genetic and molecular factors involved in the regulation and in the execution of male meiosis and spermiogenesis.

1. INTRODUCTION

Spermatogenesis is one of the most complex differentiation processes leading to sperm formation starting from an undifferentiated spermatogonial cell. The process is characterized by a series of mitotic divisions followed by meiotic divisions to form haploid spermatids and a series of post-meiotic events involving severe changes in cellular morphology that culminate in the achievement of the canonical shape of the mature sperm. The availability of *Drosophila melanogaster* mutants, that are defective for specific spermatogenesis stages, makes that insect particularly suitable for the study of spermatogenesis process. Moreover, Drosophila presents a short generation life cycle, the availability of genetic resources and a fully sequenced genome. Finally, about 61% of *Drosophila melanogaster* genes are conserved in humans (IHGSC, 2001), as it is the spermatogenesis process in terms of cells morphology and regulatory pathways.

1.1 Spermatogenesis of *Drosophila melanogaster*

Drosophila spermatogenesis occurs in testis, a blind-ended tube, in which the stages are well defined in a spatio-temporal manner from the top, containing the stem cells, to the seminal vesicle at the base where mature sperms are released. Spermatogenesis starts at the apical tip of testis in the Germinal Proliferation Center (GPC) when a germ line stem cell divides asimmetrically producing a stem cell and a gonioblast. The GPC is made up of a group of somatic cells termed the hub (H), flanked by germ line stem cells (S) each surrounded by a pair of somatic stem cells called cyst progenitor cells (CP). The germ line stem cell divides into a stem cell and a gonioblast (G) which undergoes the differentiation program. At the same time, the cyst progenitor cell divides into cyst cells (C), that enclose each gonioblast. This group of three cells is termed cyst and represent the basic unit of spermatogenesis (Fuller, 1998) (Scheme 1). The gonioblast enters the differentiation program and undergoes four mitotic divisions, forming a 16-cells cyst. Due to an incomplete cytokinesis, cyst cells

are interconnected by cytoplasmic bridges, called ring canals,. The 16 cells represent the primary spermatocytes which enters a growth phase characterized by severe morphological changes of nuclear shape.

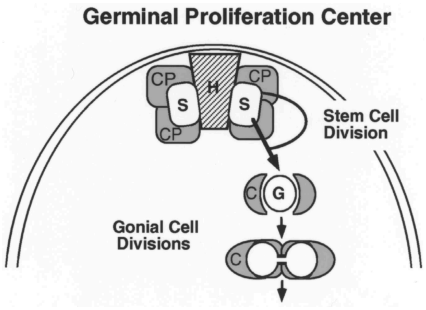

Scheme 1. Shematic rappresentation of Germinal Proliferation Center. The hub cells (H) are flanked by germ line stem cells (S) sourronded by cyst progenitor stem cells (CP). A S cell divides to form a gonioblast (G) which is sourronded by two cyst cells. (Fuller, 1998)

The growth phase can be considered as a meiotic prophase in which the cells increase their volume up to 25 times in relation with an extensive gene expression (Fuller, 1993). At that point a testis-specific gene expression occurs both for genes involved in spermatocyte differentiation and meiosis and for genes involved in late stages of spermiogenesis (Fuller, 1993) assuming the absence of post-meiotic transcription. In according with this view, all the proteins involved in spermiogenesis need to be transcribed during primary spermatocytes growth phase and stored until needed (review in White-Cooper, 2010). However, recent evidences suggested that in Drosophila, gene transcription is turned off in late primary spermatocytes and is reactivated during spermatid elongation phase when the transition between histone to protammine takes place (Barreau et al., 2008). Two groups of genes, *cup* and *comet*, are transcribed post-meiotically and do not encode sperm component proteins as in mammals, but transcripts involved in spermiogenesis as *soti,* that is required for spermatid individualization (Barreau et al., 2008). When primary spermatocytes start to growth, the nucleus assumes an eccentric position and the chromatin appears highly condensed, whereas mitochondria are positioned at the opposite pole respect to the nucleus. The polar spermatocytes show a dense network of microtubules. As the polar spermatocytes grow, chromatin subdivides into three different chromatin masses (clumps, S2 stage according to Cenci, 1994), with the progress of growth at S3 stage, the nucleus assumes again a central position and mitochondria result diffused in the cytoplasm. The two bigger chromatin masses are the somatically-paired autosomes 2 and 3, the third chromatin mass

correspond to X and Y heterochromosomes while the tiny fourth chromosomes appear as dots not always visible (Cenci et al., 1994). Spermatocytes at S3 stage are characterized by the appearance of two of the three Y chromosome loops, corresponding to the fertility factor *kl-5* and *ks-1* loci, which appear as dark spots. At S4 stage, the apolar spermatocytes increase the nuclear size, the loop *kl-3* become visible; the three loops expand and reach their maximum size at S5 stage when the spermatocyte maturation is completed. At S6 stage, the disintegration of loops marks the end of spermatocytes growth, and the chromatin starts to condense in preparation to meiotic divisions (Cenci et al., 1994). Due to the absence of meiotic recombination in *Drosophila melanogaster* males, the spermatocytes growth is considered as meiotic prophase and the homologous chromosomes association in the chromatin clumps may be a consequence of somatic pairing occurred during mitotic amplification (review by Fuller, 1993). In M1a stage the chromatin is condensed and the three major bivalents are visible while the forth bivalent is not always detectable, the asters migrate to the opposite pole and in M1b spindle fibers reach the bivalents that congregate to metaphase plate in M3 stage. At metaphase stage the chromatin appears as a unique compact mass equidistant from the poles. During the anaphase I the segregating nuclei separate and the spindle microtubules reorganized to form a dense network between the daughter nuclei called central spindle, while at the same time the number of microtubules emanating from centrosomes decrease. In telophase I the distance between daughter nuclei increases and the central spindle assumes a hourglass shape (figure 1). At the end of telophase I, the central spindle disappears and nuclei undergo the second meiotic division which resembles a mitosis (Cenci et al., 1994). Moreover, during both meiotic divisions, the mitochondria are equally distributed in segregating cells so that each haploid product of meiosis contains the same amount of mitochondria (Cenci et al., 1994). At the end of telophase II, mitochondria begin to associate with the nuclei first forming an irregular mass then, as mitochondria blend, they form a spherical structure associated with each nucleus to which is identical in shape and size. That organelle made up of fused mitochondria is called Nebenkern and the stage is referred to as “Onion Stage”, for the similarity in cross sections of the multiple membrane layers

characterizing the mitochondrial derivative with an onion (Bowen, 1922; Tates, 1971; Tokuyasu, 1975).

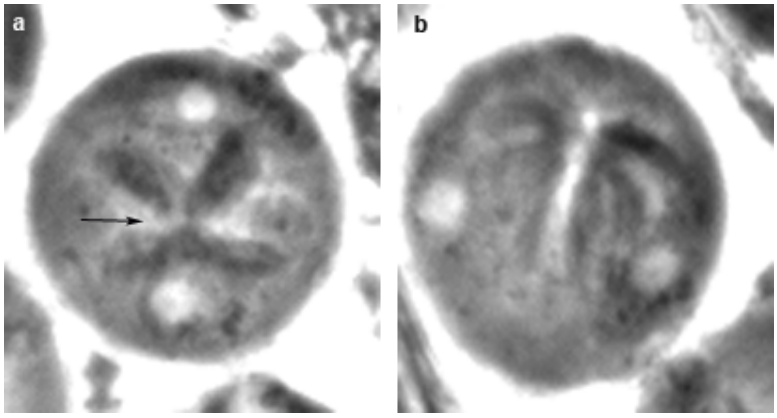

Figure 1 Meiotic telophases at light-phase microscopy. The central spindle in telophase become progressively squeezed up to assume an hourglass shape (a, arrow). At the end of telophase, the equal partition between the two newly formed nuclei of mitochondria occurs (b).

Each of the 64 haploid spermatids at onion stage are characterized by a nucleus and nebenkern in a 1:1 ratio, appearing respectively as a light and a dark masse at light microscopy (Figure 2a). The normal appearance of nucleus and Nebenkern at onion stage, in terms of both shape and 1:1 ratio, represents an indication of the correct chromosome and mitochondria segregation. Thus, an alteration of the normal situation at onion stage, allows to identify mutations that affect either karyokinesis or cytokinesis or both (Fuller, 1998) (Figure 2b).

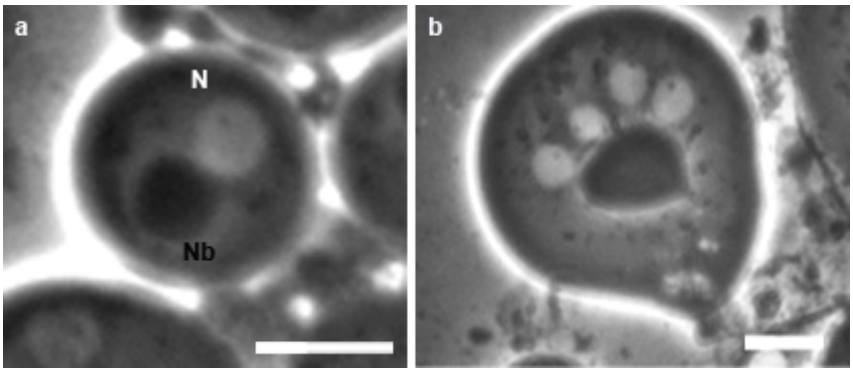

Figure 2 Onion stage and spermatids elongation at light-phase microscopy. Wildtype (a) and mutant (b) spermatids at onion stage. (a) Wildtype onion stage is characterized by one spherical nucleus (N) associated with one Nebenkern (Nb) of identical size. (b) Mutant onion stage with four nuclei associated with one big Nebenkern indicating cytokinesis anomalies. Scale bar 20um

The elongation process is the final step of spermatogenesis consisting in a series of dramatic changes involving both chromatin and Nebenkern. Each spermatid assembles flagellar axoneme from a single basal body, originating from localized centrioles at one side of the nucleus. The axoneme is a microtubule-based structure, from which the mature sperm tail originates. During Nebenkern elongation process, the wrapped layers of mitochondria membranes unfurl and two giant mitochondria aggregates elongate along the 1.8 mm of the sperm tail length (Lindsley D, Tokuyasu KT, 1980). Simultaneously, the nucleus changes its conformation from round to needle-like shape following the transition from histones to protammines leading to a higher degree of chromatin compaction (Rathke C. et al., 2007). In Drosophila three protammine-like proteins were identified, Mst35Ba, Mst35Bb and Mst77F (Jayaramaiah and Renkawitz-Pohl, 2005) and the transition to protammines is supported by transition proteins such as Tpl94D (Rathke C. et al., 2007). Each cyst of 64 mature spermatids, connected together for the incomplete cytokinesis, undergo an individualization process thanks to a cytoskeletal structure called membrane complex of individualization. This complex is formed by particular actin structures, the "investment cones" (IC), which assemble at the head/tail boundary of each spermatid and then move downward along the spermatid tail. Under the investment cone action most of the cytoplasm is pushed in a sort of "bag for waste", causing a dilation of the cyst which leads to the release of the 64 individualized sperms (Fabrizio et al., 1998). Finally, sperm tail coils and the sperms are released into the seminal vesicle where they acquire mobility.

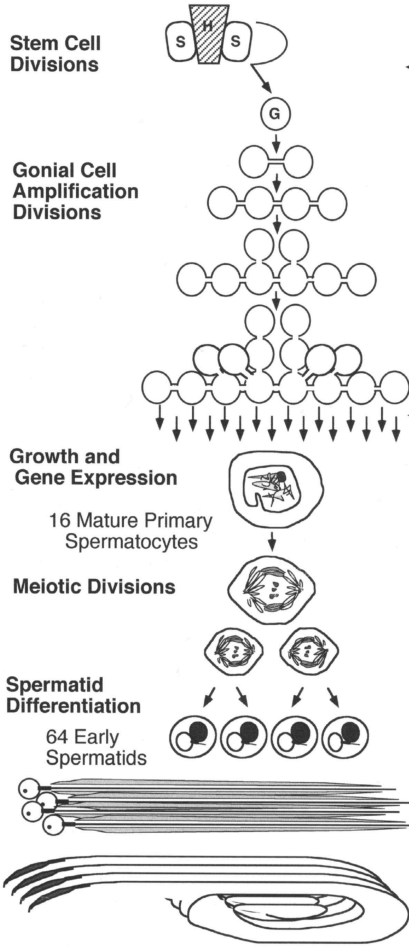

Scheme 2. *Drosophila melanogaster* spermatogenesis. Germ line stem cell divides into a stem cell and a gonioblast (G) which undergoes to a series of four mitotic divisions forming a 16-cells cyst interconnected by cyplasmatic bridges. The 16 primary spermatocytes enter in growth phase. At the end of growth phase, 16 primary spermatocytes meiotically divide to generate a 64 cells cyst of haployd spermatids at onion stage. At onion stage, each spermatid constist of a phase-light spherical nucleus associated with a phase-dark organelle of aggregated mitochondria called Nebenkern, in a 1:1 ratio. During the elongation phase, spermatids assembled and individualize the sperm tails, chromatin condenses to form a needle-shape heads of mature sperms. (Fuller, 1998)

1.2 Genetic control of *Drosophila melanogaster* spermatogenesis

The differentiation process of spermatogenesis that starts from a germinal stem cell and ends with the formation of mature sperms requires a finely regulated gene expression. The gene expression during spermatogenesis must be strictly governed to ensure normal cellular differentiation to generate functional gametes. The analysis of mutants affecting different stages of spermatogenesis revealed that there are three critical regulatory points during germline male differentiation: firstly, the choice between stem cell renewal and spermatogonial differentiation; secondly, the switch to the meiotic divisions at the end of mitotic amplification; thirdly, the transition from primary spermatocytes to meiotic division program (transition G2/M of cell cycle). The molecular pathway of first checkpoint has not been yet clarified. It has been noted that the cell maintaining

contact with the hub tends to maintain stem cells identity while, the cell displace away from the hub undergo to differentiation program. The apical hub cells express protein from *armadillo* locus as Fasciclin III, D-Ecadherin and β-catenin (Peifer et al., 1993) and *hedgehog* gene encoding a signaling molecules (Lee et al., 1992), suggesting a role of the hub as signaling center (Fuller, 1998). One of the pathways implicated in stem cells differentiation involves the JAK-STAT signaling activation as a consequence of Upd ligand secretion (Kiger et al., 2001; Tulina and Matunis, 2001). The transition between sparmatogonial mitotic divisions to the primary spermatocytes growth and consequently the trigger of meiotic program is regulated by two genes, *bag of marbles* (*bam*) and *benign gonial cell neoplasm* (*bgcn*). Mutant testes for both genes are full of cysts of germ cells and completely lacking of primary spermatocytes or downstream stages. The correct function of *bam* and *bgcn* are mandatory to ensure the transition to the onset of meiotic differentiation program (review by Fuller, 1998). The third checkpoint, the transition between the growth period of primary spermatocytes that can be considerate as an extended G2 phase, to the entry in meiosis I is regulated by two different classes of genes, "meiotic arrest class" and "twine class". Spermatocytes of "meiotic arrest" mutant do not enter into meiotic divisions and do not execute post meiotic spermatids differentiation.
The meiotic arrest class can be subdivided in two subclasses on the basis of different phenotypes, *always early* (*aly*) class and *cannonbal* (*can*) class (White-Cooper., 1998).

can class includes the following genes: *cannonbal* (*can*) (Hiller et al., 2001), *meiosis I arrest* (*mia*) (Hiller et al., 2004), *spermatocyte arrest* (*sa*) (Hiller et al., 2004) and *no hitter* (*nht*) (Hiller et al., 2004) which respectively encode for a testis specific TBP-associated factors (tTAFs) TAF-5, TAF-6, TAF-8 and TAF-4 playing a role in the interaction between RNA polymerase II and gene promoter regions. The basal transcription factor complex, TFIID, which is constitute by TATA-binding protein and (TBP) and several TAFs, is an ubiquitous transcriptional factor always acting during transcriptional process. The discovery of testis specific TAFs led to a model in which they can act as basal transcription factors for promoters of genes required in spermiogenesis (White-Cooper, 2010). Moreover, the colocalization of TAFs with PRC1, a

component of Polycomb repression complex (Chen et al., 2005) led to hypothesize a "repressor of a repressor" pathway according to which tTAFs sequester the PRC1 repressor away from testis-specific promoters allowing gene expression (White-Cooper, 2010).

aly class includes the following genes: *always early* (*aly*) (White-Cooper et al., 2000) whose molecular functions is unknown and *lin-9* is its homolog in *C.elegans*, *cookie monster* (*comr*) whose molecular function is unknown (Jiang and White-cooper, 2003), *tombola* (*tomb*) encoding for a DNA binding protein and *lin-54* is its homolog in *C.elegans* (Jiang and White-cooper, 2007), *matotopetli* (*topi*) (Perezgazga et al., 2004) and *achintya* and *vismay* (*achi-vis*) (Ayyar et al., 2013; Wang and Mann 2003) encoding for DNA binding proteins. *aly* gene is conserved from plants to animal, except in fungi (White-Cooper et al., 2000) and it is a paralog of *mip130* gene. Mip130 protein, together with Rbf, E2F2, Dp is a subunit of dREAM/MMB repress gene expression complex (Lewis et al., 2004). An analogous dRAM/MMB complex and specific for testis, named testis meiotic arrest complex (tMAC) has been identified in Drosophila (Beall et al., 2007). Some of the tMAC components are in common or are paralogs of dRAM/MMB complex subunits, others as Comr and Topi are unique of tMAC ensuring a testis specific gene activation (White-Cooper, 2010). Even if dREAM complex is linked with transcriptional inactivation, the role of *aly* genes is presumably that of transcriptional activators rather than repressor of a repressor due to their localization, which determine their function, with euchromatin in primary spermatocytes (White-Cooper, 2010, Jiang and White-cooper, 2003, Wang and Mann 2003, Jiang et al., 2007).

Spermatocytes of ***twine-class*** mutants skip one or both meiotic divisions and some peculiar events of meiosis as spindle assembly, chromosomes segregation and cytokinesis, but spermatids differentiation, although with defects, proceed. The *twine-class* includes *Dmcdc2*, *twine* (*twe*), *pelota* (*pelo*), *boule* (*bol*) genes and are required for entry into meiotic cell divisions. Studies showed that the meiotic factors involved in entry into meiosis are the same involved in mitotic cycle. The cdc2 kinases is responsible for the initiation of mitosis, the activity of cdc2 is regulated by its association with cyclin and with the phosphorilation

of threonine 167 in *S. pombe* (reviewed by Nurse, 1990). The cdc2 kinases activity is repressed by phosphorilation of tyrosine 15 in S. pombe (Gould et al., 1990) and threonine 14 in higher eukaryotes (Krek and Nigg, 1991; Norbury et al., 1991) by Wee1. The removal of the inhibitory phosphates is mandatory for the activation of cyclin/cdc2 activation and consequently for the beginning of M phase (reviewed by Maines and Wasserman 1998); the inactivation of cyclin/cdc2 complex for the M phase exit occur by cyclin degradation (Glotzer et al., 1991). Phosphatases belong to cdc25 family remove the inhibitory phosphates of cdc2 (Dunphy and Kumagai, 1991; Gautier et al., 1991; Strausfeld et al., 1991). In Drosophila have been identified two cdc25 phosphatases, String is active in mitosis and cdc25 homolog Twine which are responsible for the onset of the meiotic divisions (Edgar and O'Farrel, 1989, 1990; Jimenez et al., 1990; Alphey et al., 1992; Courtout et al., 1992). *Dmcdc2* encodes for cdc2 kinase which form a complex with Cyclin B underline the transition G2/M, the activity of that complex is mediated by a phosphorilation/dephosphorilation of the cdc2 kinase (reviewed by Nurse, 1990). *twine* and *Dmcdc2* are required for the transition G2/M during Drosophila spermatogenesis (White-Cooper et al., 1993; Eberhart and Wasserman, 1995). Mutation in *twine* leads to sterility but does not affect somatic development and viability, pre-meiotic stages of spermatogenesis are phenotipically normal while chromosomes condensation is incomplete, cyclin A is not degraded, centrosomes do not separate and spindle does not form. *Dmcdc2* mutations leads to developmental defects and larval lethality suggesting a role also in mitosis (Stern et a., 1993). Mutants for *twine* and *Dmcdc2* accumulate cysts of 16 undivided nuclei however, many aspects of post meiotic stages, as elongation of spermatids, still occur leading to the formation of unbalanced and no motile sperms (White-Cooper et al., 1993). *twine* gene is transcribed early during the extended G2 phase therefore, *twine* mRNA accumulation, is not sufficient to promove the G2/M transition contrary with that observed with the transcription of *string/cdc25* that trigger the G2/M transition (Edgar and O'Farrel, 1989, 1990). POLO kinase activates TWINE consequently triggering CyclinB/cdc2 complex. Once activated the CyclinB/cdc2 complex activates by phosphorilation TWINE (its same activator) and repressed its same inhibitor Wee1 by a positive feedback loop. *pelota* and *boule* show a similar phenotypes observed in *twine* and *Dmcdc2,* they fail some

meiotic aspects as chromosomes congression, nuclear lamina breaks down and spindle formation but exhibit post-meiotic differentiation (Eberhart and Wasserman, 1995; Eberhart et al., 1996). *boule* encodes for a RNA-binding protein, it is expressed only in testis and mutation in the gene affect only meiosis (Eberhart et al., 1996). *pelota* is widely express and acts both in mitosis and in meiosis (Eberhart and Wasserman, 1995). Finally, *Dmcdc2*, *twine* and *roughex*, have a role in regulating the second meiotic division. *roughex* in particular negatively regulates MII, an excess of *rux* prevents the second meiotic division, an low level of *rux* leads to an extra MII division (Gonczy et al., 1994). A model for meiotic cell cycle and spermatid differentiation control cordinating by both *meiotic-arrest* and *twine* gene clesses has been proposed (Fuller, 1998). *aly* gene could play a role as global regulator of spermatogenesis inasmuch *aly* control the transcription or the activity of *can*, *mia* and *sa* and *twine*, *cyclinB* and *boule* or their products (White-Cooper., 1998). In *can*, *mia* and *sa* mutants a primary spermatocytes arrested in G2/M phase were observed suggesting that all the genes involved in spermatids differentiation has to be transcribed. Moreover, in *twine* mutant the *twine* mRNA is present but protein can be not trasleted or not stabilized (White-Cooper., 1998). The hypotesis is that a gene/genes regulate by *meiotic-arrest* class genes can act to regulate and stabilize TWINE protein (Fuller., 1998).

1.3 RAE1: structure and functions

The WD domain containing proteins belongs to a family characterized by a common sequence repeat enriched of tryptophan (W) and aspartic acid (D) usually at the end of a 40 residues sequence. The WD domains show a beta propeller fold. WD proteins are found in all eukariotes and show a very wide variety of functions: they are involved in signal transduction, RNA processing, chromatin assembly, vesicular trafficking, cell cycle progression and many others. A common feature of WD proteins seems to be the ability of interacting with different proteins to form complexes (for a review see Smith, 2008). RAE1 is a conserved component of WD-40 protein family (Neer et al., 1994) showing several different functions. RAE1 was first identified in *Schizosaccharomyces pombe* (spRae1p) in a screening for temperature-sensitive mutation defective for RNA exportation from nucleus to cytoplasm. *rae1* (ribonucleic acid export 1) mutant accumulates poly $(A)^+$ RNA in the nucleus together with defects associated with organization of actin and tubulin pattern and a block at the G2/M transition in mitosis (Brown et al., 1995). Moreover, when *rae1* is inactivated or depleted the cells arrest in G2 phase without the formation of mitotic spindle (Whalen et al., 1997). In *Saccharomyces cerevisiae*, the *S.pombe rae1* homolog, *gle2,* is associated with nuclear pore complexes. *gle2* mutants show an accumulation of poly $(A)^+$ RNA and a severe perturbation of the structure of nuclear pore complexes and of nuclear envelope but, contrary to what observed in *S.Pombe*, *gle2* is required but not essential for cells proliferation (Murphy et al., 1996). The role of RAE1 in the process of mRNA trafficking between nucleus and cytoplasm has been demonstrated also in human. The human protein RAE1 is involved in nuclear cytoplasmic mRNA export (Bharathi et al., 1997) by its direct binding through the GLEBS-like motif to NUP98 at nuclear pore complex (Pritchard et al., 1999). In mammalian cells, GLEB motif modulates also the binding of hRAE1 (and mRAE1) to the mitotic checkpoint protein mBUB1 indicating an interaction between nuclear cytoplasmic trafficking and mitotic machinery and a role for RAE1 as mitotic checkpoint regulator (Wang et al., 2001). Knock-out mice for *rae1* and *bub3* show mitotic checkpoint defects and chromosome missegregation, but the lack of *rae1* has no effects on mRNAs export (Babu et al., 2003). Moreover, Rae1 and Nup98 are

associated with APC and regulate the transition from metaphase to anaphase in mammalian mitotic cells (Jeganathan et al., 2005). In Xenopus egg extracts, RAE1 binds to microtubules and is involved in the spindle assembly regulating the activity of the spindle-assembly factor Ran. In HeLa cells the interaction between the Nuclear Mitotic Apparatus protein (NuMA) and RAE1 was demonstrated showing that a perturbation of protein levels lead to the formation of spindle defects and consequent chromosome alignment anomalies. The equilibrium of the two proteins is a critical condition for bipolar spindle formation (Wong et al., 2006). In *Drosophila melanogaster* the role of *rae1* was firstly investigated in SL2 culture cells. The dmRae1 protein localizes at nuclear envelope and shows a higher identity with the human form than with the yeast form . The depletion of *rae1* by a dsRNA interference does not affect the mRNA export but an accumulation of cells in G1 phase and defects in S phase entry were observed. Those evidences indicates that in drosophila culture cells dmRae1 is not involved in nucleocytoplasmic trafficking but is involved in the progression of the cell cycle through the regulation of G1/S transition (Sitterlin 2004). From those observations the pleiotropic effects of the *rae1* gene emerge that leads to a multiple protein roles among organisms. Further insights onto the pleiotropic effects of *rae1* arise from Drosophila *in vivo* studies, from which both an involvement in the regulation of neurogenesis and a role in meiotic cell cycle emerge (Tian et al., 2011; Volpi et al., 2013). The ubiquitin ligase *Highwire* is a member of conserved PHR proteins that regulates the development of nervous system. Drosophila *hiw* mutants show an abnormal overgrowth of synapses at larval neuromuscolar juction (NMJ) in terms of number and size of boutons and extension of branches (Hong et al., 2000). Using the tandem affinity purification assay *Drosophila* Rae1 was identified as interactor of Hiw (Tian et al., 2011 Like *hiw* mutant, *rae1* mutant flies show terminal synapsis overgrowth and small boutons. Further evidences of the interaction between *rae1* and *hiw* arise from the fact that the heterozygosity conditions of *rae1* can enhance the phenotype observed in a *hiw* ipomorfic mutant indicating that the two genes collaborate to control the terminal synapsis overgrowth (Tian et al., 2011). Finally, the authors show that RAE1 regulates in a positive manner the level of E3 ubiquitin ligase Hiw to restrain the growth of terminal synapsis (Tian et al., 2011). An interaction of RAE1 with RPM-1,

orthologue of Highwire, that regulate the axon termination and synapse formation, was shown in *C. elegans* putting in evidence a conserved role between species of RAE1 as regulator of neuronal development (Grill et al., 2012). The role of *rae1* in meiosis was shown in a study aimed to characterize a male sterile recessive mutation of *Drosophila melanogaster* (Volpi et al., 2013). *rae1* mutant males are sterile but completely viable, the meiocytes do not complete meiosis I and do not progress towards meiosis II, but the unreduced spermatids progress to the final stages of spermatogenesis although producing defective sperms. Cytological analysis showed defects in chromatin condensation from pre-meiotic stage up to metaphase I division where chromosomes were poorly organized and chromatin fragments are delocalized respect to metaphase array ending with chromosome lagging in ana/telo phase. The meiotic spindle is poor of microtubules and the central spindle is mislocalized. Defects associated with actin structures and centrioles distribution were also observed (Volpi et al., 2013). Those evidences emphasized the multifaceted role of RAE1 as protein involved in both the mitotic and the meiotic cell cycle.

1.4 Nuclear Lamina: Structure and Functions

The nuclear envelope (NE) is a cellular ultrastructure that encloses the genetic material in eukaryotic cells. The NE consists of an outer membrane, in continuity with the endoplasmic reticulum, and an inner membrane overlooking the nuclear lumen. In eukaryotes, the inner surface of the NE leans over a network of filamentous proteins called nuclear lamina (NL) and made up by lamins (Figure 3).

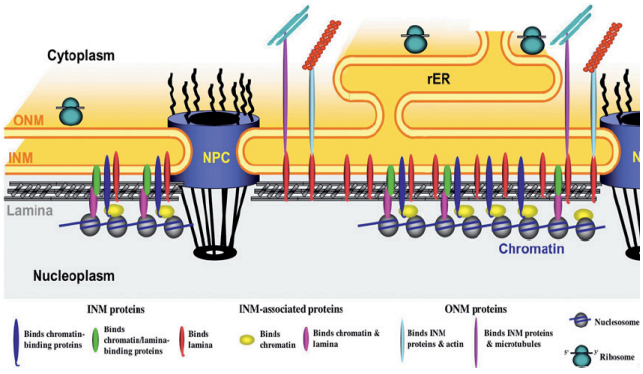

Figure 3 Nuclear envelope structure. The nuclear envelope is made by two layers, the inner nuclear membrane (INM) and the outer nuclear membrane (ONM) in continuity with the endoplasmic reticulum and nuclear lamina. The double membrane layer is crossed by the nuclear pore complexes (NPC) allowing the membrane trafficking of proteins and mRNAs.

La The inner membrane contains a set of proteins mainly necessary for anchoring the chromatin and nuclear lamina. The nuclear lamina, a fibrous membrane of 15nm made by lamin proteins, located beneath the INM, provides a mechanical support to the nuclear envelope determining the overall shape of the interphase nucleus. (D'Angelo and Hetzer., 2006)

Lamins are members of V type intermediate filament (IF) family and show the canonical structure of intermediate filaments. They are characterized by a globular amino-terminal domain (head domain), an internal α-helix central rod domain and a longer carboxy-terminal domain (tail domain) containing a conserved structural motif similar to the immunoglobulin fold (Ig-fold) and a –CAAX box involved in post-tradutional modifications to obtain mature proteins. A nuclear localization sequence (NLS) is present between the tail domain and the central rod domain allowing the protein transport into the nucleus (Figure 4). The α-helix domain is necessary to form the coiled-coil dimers, which associate in a head-to-tail manners to form tetrameric protofilaments. The interaction of protofilaments forms the 10nm filaments. The nuclear lamina is a polymer made up of a single layer of filaments (for reviews see Dechat et al., 2008 and 2010).

Figure 4 Structure of pre-lamin. At the beginning lamins are expressed as pre-lamins showing the following structure: α -helix central rod domain in red, the Nuclear Localization Sequence in grey (NLS), the Ig-fold in blue and the –CAAX sequence at C-terminal. (Dechat et al., 2008)

Lamin proteins are subdivided in A- type, expressed in a controlled manner during development, and B-type lamins, ubiquitously expressed and essential for cellular life. Invertebrates have only one lamin gene encoding for B-type lamins, except Drosophila that has two lamin genes, *lamDm0* encoding for a B-type lamin, and *lamC* encoding for an A-type lamin. *lamin Dm0* is expressed during oogenesis, early embryonic development and in tissue cultures (Smith et al., 1987; Smith and Fisher, 1989). Lamin Dm0 protein is synthesized in the cytoplasm and immediately processed to Lamin Dm1 by proteolytic process. Lamin Dm1 is subsequently assembled in the nuclear lamina and where two different phosphorylations events take place, determining the formation of Lamin Dm2 isoform. Lamin Dm1 and Lamin Dm2 are in equilibrium during cell growth (Smith et al., 1987). During meiosis and mitosis when nuclear envelope breaks down, a conversion of these two isoforms by phosphate rearrangement in a third soluble isoform, called LaminDmmit takes place leading to the disassembly of the nuclear lamina (Smith and Fisher, 1989). Contrary to what observed in mammals, in Drosophila the nuclear lamina assembly/disassembly is guided by a rearrangement of phosphate positions and not a change in global level of phosphates (Smith and Fisher, 1989). In mammals there are three genes for lamins, *LMNA*, *LMNB1* and *LMNB2*, that undergo alternative splicing to generate 7 different isoforms. The A, A Δ 10, C and C2 lamins are transcribed from *LMNA* gene and are called A-type lamins (Fisher et al., 1986; McKeon et al., 1986; Furukawa et al., 2003); the B1 lamin is transcribed from the gene *LMNB1* and the B2 and B3 lamins are transcribed from LMNB2 gene and are as a whole defined B-type lamins (Pollard et al., 1992; Bia et al., 1992). The vertebrate cells express at least one of the B-type lamins, whereas the isoforms A, A Δ 10, and C are developmentally regulated and are mainly expressed in

differentiated cells (Rober et al., 1989; Machielis et al., 1996); the C2 and B3 isoforms are expressed only in the germ line (Fukurawa and Hotta, 1993; Fukurawa et al., 1994; Alsheimer et al., 1999). Due to the main function of nuclear lamina (NL) to provide support to the nuclear envelope, during the cell cycle the nuclear lamina undergoes structural changes. The most significant alteration of nuclear lamina takes place during the transition prophase to metaphase of mitotic cells, when the nuclear envelope breaks down. At this stage nuclear lamina disassembles by phosphorylation of residues flanking the rod domain leading to a depolymerization of lamins polymers. The nuclear lamina reassembly is guided by dephosphorilation of the same residues (for a review see Moir et al., 2000). The NL contributes to maintain the mechanical properties of the cell forming a bridge between the nucleus and the cytoplasm and is involved in determining the nuclear shape (for a review Moir et al., 2000; Dechat et al., 2010;). Due to the nuclear lamina position very close to chromatin, a role of lamins in regulations of gene transcription through chromatin positioning has been suggested. Microscopy studies demonstrated the association between heterochromatin and nuclear lamina (Paddy et al., 1990; Fawcett, 1996) and the interaction of lamins with histones and specific DNA sequences was reported (for a review Dechat et al., 2010). A decrease in the expression of *lamDm0* in drosophila blocks the nuclear membrane assembly (Lenz-bohme et al., 1997) and the down regulation of lamin gene leads to chromatin condensation and chromosome segregation defects in *C.elegans* (Liu et al., 2000). Lamin involvement in DNA replication and in transcription was also suggested: in culture cells, lamin B1 localized at replication foci (Moir et al., 1994) and lamin depletion in Xenopus egg extracts results in a block of DNA replication without effects on nuclear envelope behavior although nuclei are smaller (Newport et al., 1990). Moreover, the association of lamin proteins with DNA replication factors as PCNA was shown (Shumaker et al., 2008). Lamins also have a role in the control of gene expression by controlling the nuclear chromatin organization. Evidences showed that inactive genes are often allocated close lamina region, it was thus suggested that nuclear lamina could act to assemble a transcriptionally silent domain interacting directly with chromatin (for a review see Dechat el al., 2010). In *Drosophila melanogaster* specific chromosomal regions of inactive chromatin are associated with nuclear

envelope (Mathog and Sedat, 1989). Moreover, changes in lamin expression lead to histone modification alterations and consequently changes in chromatin structure, thus pointing out a role of lamins in epigenetic regulation. Finally, lamins are involved in cell cycle regulation , acting in pathways involved in cell cycle progression (for a review see Dechat et al., 2010). By all these evidence is clear, therefore, that the nuclear lamina has not only a role in determining the architecture of the nucleus but it is also actively involved in gene regulation and hence in the control of nuclear and cellular process.

2. AIM OF THE PROJECT

The proper execution of spermatogenesis process, from stem cell divisions to mature sperms formation, is a mandatory condition to ensure male fertility. *Drosophila melanogaster* is a widely used model organism to genetically and cytologically dissect developmental processes. Drosophila male sterile mutations affecting any stages of spermatogenesis represent an excellent study material to explore the genetic mechanism regulating the whole process. Due to the conservation of developmental mechanisms between species, evidences obtained in flies should provide insight into genetic and molecular pathways underpinning male fertility in other organisms, including humans. The general aim of my PhD research project was the analysis of *ms(2)Z5584* and *ms(2)Z1168* mutant strains belonging to a unique collection of 13 ethyl-methansulfonate (EMS)-induced male sterile recessive mutants on chromosome 2 and 3 identified in a large screening of male-sterile mutations (Wakimoto et al., 2004). Preliminary cytological screen of mutations highlighted a general and common aberrant phenotype affecting the entry into the meiotic cell cycle. In particular mutants skip one or both the meiotic divisions but carry out the spermatid differentiation, although with anomalies,. That phenotype reminds that observed in *twine* class mutants.

The *ms(2)Z5584* mutant strain was previously characterized both genetically, by identifying a point mutation in *rae1* gene, and cytologically by a description of aberrant phenotypes throughout the spermatogenesis process (Volpi et al., 2013). Starting from those evidences, I first confirmed the identification of *rae1* as the gene underling the *ms(2)Z5584* mutant phenotype. The *rae1* gene was knocked-down by RNA interference and the ensuing phenotipic effects on spermatogenesis were analyzed and compared to *ms(2)Z5584* mutant defects. Secondly, the RAE1 localization pattern during meiotic cell cycle was investigated by GAL4/UAS system allowing the expression of *UASGFP-rae1* transgene under either a testes-specific or a constitutive driver. Finally, a *ms(2)Z5584* mutant phenotype rescue was performed using an *UASGFP-rae1* transgene.

The *ms(2)Z1168* mutant strain was previously partially characterized. Preliminary recombination and deficiency mapping allowed to identify the genetic region containing

the mutation. I carried out a complete characterization of the mutant phenotype during spermatogenesis. The analysis was performed by immunohistochemestry technique using antibodies against several structures involved in male meiosis and confocal microscopy. The *ms(2)Z1168* mutant exhibited anomalies in nuclear lamina structure together with chromatin condensation defects. The genetic region containing the *ms(2)Z1168* mutation was further restricted by recombination and deficiency mapping. The gene identification was made by genetic approach using RNA interference and by sequencing.

3. RESULTS AND DISCUSSIONS

3.1 *ms(2)Z5584* mutant strain: the background

The *ms(2)Z5584* mutant strain belongs to a unique collection of 13 ethyl methansulphonate induced male sterile recessive mutants on chromosomes 2 and 3 (Wakimoto et al., 2004). The general phenotypes of that collection remind to that observed in *twine* class mutants. The *ms(2)Z5584* mutation complemented *twine* so a possible allelism between the two genes was previously excluded. The *ms(2)Z5584* mutant was widely characterized both cytologically and genetically (Volpi et al., 2013). The *in vivo* cytology pointed out hernias in primary spermatocytes, aberrant onion stages and round and unpolarized nuclei in sperm bundles. Indirect immunofluorescence indicated chromatin condensation defects, chromosome misalignement at metapahse plate, compromised meiotic spindle, and altered actine structures and centriole behavior (Figure 5). By recombination and complementation mapping the genetic locus containing the *ms(2)Z5584* mutation responsible of the observed phenotype was identified. A point mutation in the open reading frame of *rae1* gene was identified by sequencing. The mutation give rise to a G/C to A/T substitution leading to a substitution of a glycine (G) with an acid aspartic (W) residue at position 129, which is invariant from yeast to mammals and is located within a highly conserved 12 amino acid sequence of the third WD-40 repeat domain.

From this starting point started my research work aimed to unequivocally demonstrate that *rae1* is the gene responsible of the observed phenotype in *ms(2)Z5584* mutant strain and to assess the subcellular localization of RAE1 during spermatogenesis.

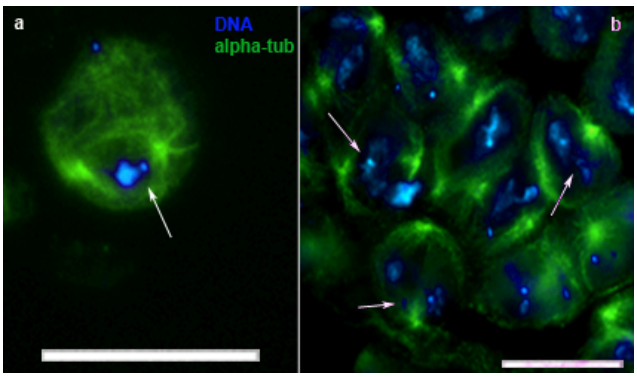

Figure 5 *ms(2)Z5584* homozygous mutant defects. DNA (DAPI staining) in blue, meiotic spindle (alpha-tubulin staining) in green. Meiotic metaphases showing chromosome lagging at metaphase plate (a and b arrows) and chromatin condensation defects (b). Note in both (a) and (b) that the meiotic spindle results poor of microtubules. Scale bar 20 μn.

3.2 Sterility and meiotic and spermiogenesis defects in *rae1* RNA-interfered males

RNA interference tool allows to inactivate a specific gene. The availability of an inducible UAS-RNAi construct against *rae1* gene allowed us to selectively knock down the gene in the testes using a GAL4 construct under a testis-specific promoter. This experiment was aimed to compare the *rae1* silenced phenocopy to the *ms(2)Z5584* mutant phenotype. The r*ae1* RNAi construct was induced by a germline specific *BamG4UASDicer2* driver according to the cross scheme in figure 6.

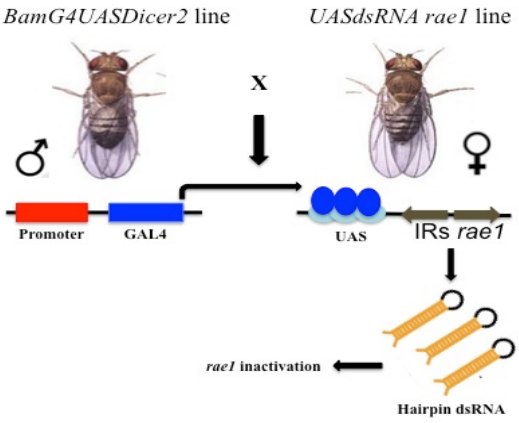

Figure 6 GAL4/UAS System for RNAi induction. Gal4/UAS system is a very powerful tool allowing the tissue specific gene silencing. The yeast GAL4 transcription factor binds the ***U***pstream ***A***ctivating ***S***equence and activates the expression of dsRNA hairpin. In Drosophila the two parts of the system are carried by two different fly lines, a GAL4 line containing a driver that provide GAL4 expression and a line carrying specific gene fragments as inverted repeats downstream of the UAS activation domain.

BamG4UASDicer2 is a testis-specific driver that drive the *ds*RNA interference from late spermatogonia to early spermatocytes by the expression of GAL4 protein that recognized the UAS sequence upstream the IRs (inverted repeats) of *rae1* gene (White-Cooper, 2012). Moreover, the strength of the interference is increased by the presence of *Dicer2* that expresses more DICER proteins than the endogenous one. I previously tested the fertility of the *rae1* interfered males and found that they were fully sterile. Then, the *rae1* interfered males were fixed, immunostained by anti-alpha tubulin antibody to detect meiotic spindle and anti-Spd2 for centrosomes, and stained by DAPI to visualize chromatin. To test whether the observed phenotype in *ms(2)Z5584* mutants was comparable to that obtained with RNA interference, I focused on meiotic divisions to appreciate both the chromatin and meiotic spindle defects. In figure 7 I summarized the phenocopy meiotic defects that strongly resemble to those observed in *ms(2)Z5584* homozygous (compare figures 5 and 7). The dividing cells are characterized by abnormal metaphase plates showing misaligned and lagging chromosomes (Figure 7 b,c,d arrows) together with an unbalanced distribuition of chromatin that is also positioned out of the spindle axes (Figure 7, b, arrow) and d arrowhead. At anaphase,

daughter nuclei often showed an unbalanced chromatin content, and the meiotic spindle resulted poor of microtubules and a definite central spindle was never visualized (Figure 7a, arrows).

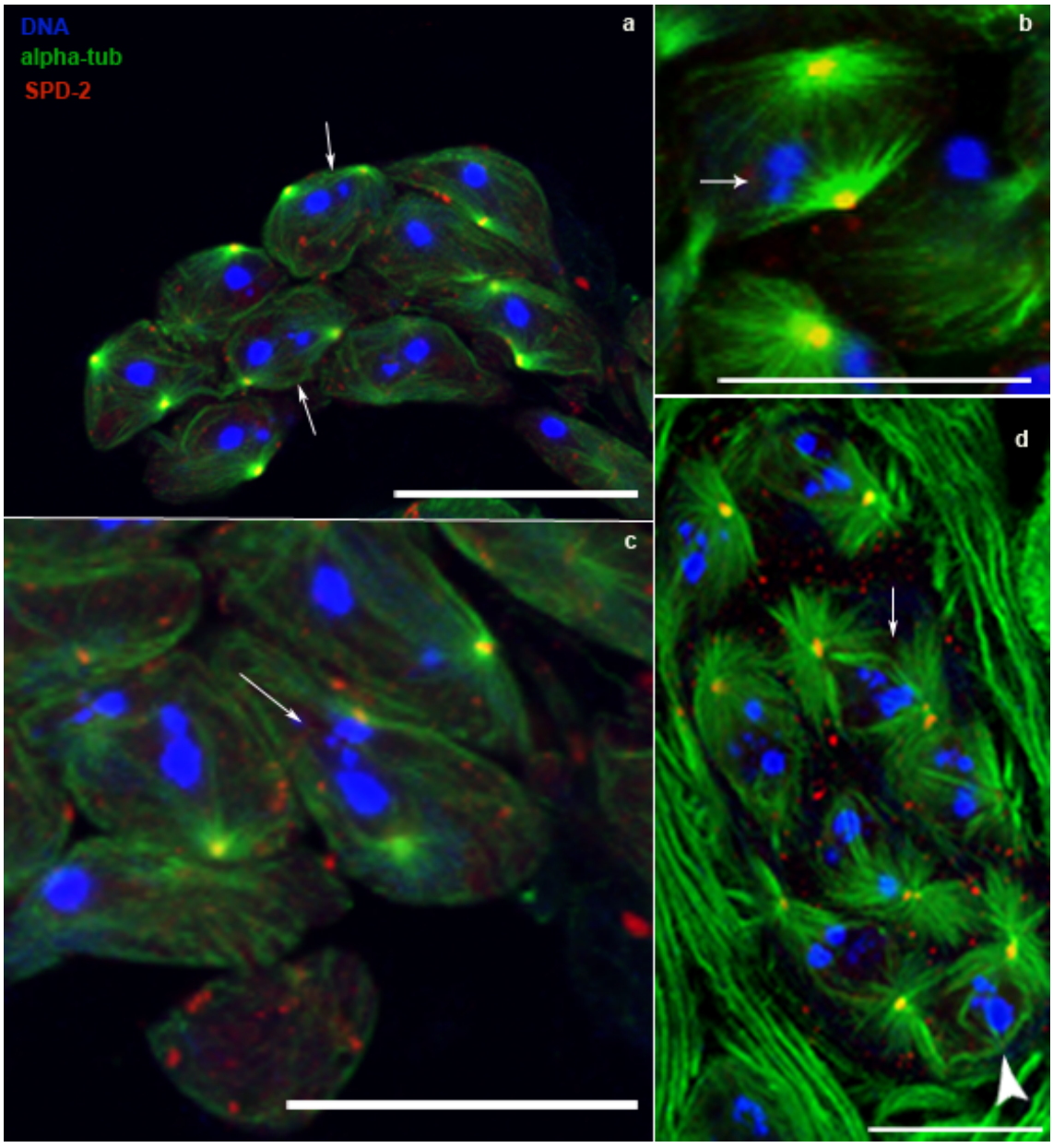

Figure 7. Confocal microscopy analysis of *rae1* dsRNA meiotic defects. DNA (DAPI staining) in blue, meiotic spindle (alpha-tubulin staining) in green, centrosomes (SPD-2 staining) in red. (a-d) Metaphases and anaphases of the first meiotic division. Unbalanced chromosomes segregation and lagging chromosomes are shown (arrows). Scale bare 20 μn.

The sterility of *rae1* knock-down flies and the similarity of their cytological phenotype with that of *ms(2)Z5584* mutants, led me to conclude that *rae1* is the mutated gene responsible of the phenotypes observed in *ms(2)Z5584* homozygous mutants. Thus.

rae1 plays a fundamental role in the execution of a proper meiosis and spermatogenesis. Due to meiotic chromosomes segregation defects characterizing the *ms(2)Z5584* mutant, it is reasonable to speculate a role of *rae1* in chromosome segregation as previously observed in mitosis. *Rae1* haplo-insufficient mice show significant chromosome missegregation defects which increase in combination with a *Bub3* deficit. This suggests a cooperation of the two proteins for proper chromosome segregation in a common pathway involving also the mitotic checkpoint control protein BUB1 (Babu et al., 2003; Basu et al., 1999). The localization of RAE1, BUB1 and BUB3 at mitotic unattached kinetochores (Wang et al., 2001; Babu et al., 2003) could generate a wait signal in metaphase before skipping to anaphase (Babu et al., 2003). During Drosophila spermatogenesis BUB1 results associated with kinetochores at prometaphase I cells, decrease during metaphase I and disappear during anaphase I moreover, *bub1* mutant show chromosomes missegregation defects (Basu et al., 1999). An equivalent of the spindle checkpoint in *Drosophila* meiosis seems to exist even though less efficient than the mitotic one. It has been conjectured an involvement of the Bub1 pathway in the delay, but not full arrest, of the meiotic cell cycle also in the presence of unattached chromosomes (Basu et al., 1999). A reduced severity of the meiotic spindle checkpoint is also supported by my findings in the *ms(2)Z5584* mutants which progress to the final stages of spermatogenesis notwithstanding the severe meiotic defects. In the light of this view and considering the colocalization of RAE1 and BUB1 in mitosis, I can likewise speculate a colocalization of the two proteins at kinetochores of meiotic chromosomes and their synergistic involvement in meiosis spindle checkpoint. Moreover, in eukaryotic cells the proper chromosome segregation is guaranteed by a bipolar spindle formation. In HeLa cells the interaction between RAE1 and NuMa protein are responsible for a correct formation of mitotic spindle (Wong et al., 2006). The presence of meiotic spindle anomalies *ms(2)Z5584* mutant and in *rae1* interfered males could likewise suggest the interaction between RAE1 and proteins involved in meiotic spindle formation (Volpi et a., 2013).

3.3 Confocal analysis of GFP-RAE1 localization during spermatogenesis

By confocal microscopy analysis I followed RAE1 localization pattern during wildtype spermatogenesis in *Drosophila melanogaster*. As above reported, the GAL4/UAS system is composed by two different fly lines, a GAL4 line containing a *Bam* or a *Tubulin* driver that provide, respectively, testis-specific or constitutive GAL4 expression, and a reporter line carrying a coding sequence of targeted gene with a GFP reporter gene fused to the *rae1* sequence, downstream of the UAS activation domain (see scheme in figure 6 paragraph 3.2). In these experiments, I followed the RAE1 distribution through the whole spermatogenic process, from mitotic stages to mature sperms, taking advantage of GFP protein autofluorescence .

3.3.1 GFP-RAE1 localization under the control of *BamG4* driver

Figure 8a shows the chromatin staining of a testis apex. The GFP-RAE1 signal was not detectable at the top (Figure 8 a' and merge) due to the activity of BamG4 driver that starts at late spermatogonial stage. The GFP-RAE1 was distributed in all nuclei as a rim at nuclear periphery from young to mature spermatocytes (Figure 8 a', b' and merge). The greater intensity of the GFP-RAE1 signal around some nuclei and in the cytoplasm that was visible in the median part of the testis corresponded to young polar spermatocytes, and was presumably due to the BamG4 driver expression peak (Figure 8 a' and Figure 9).

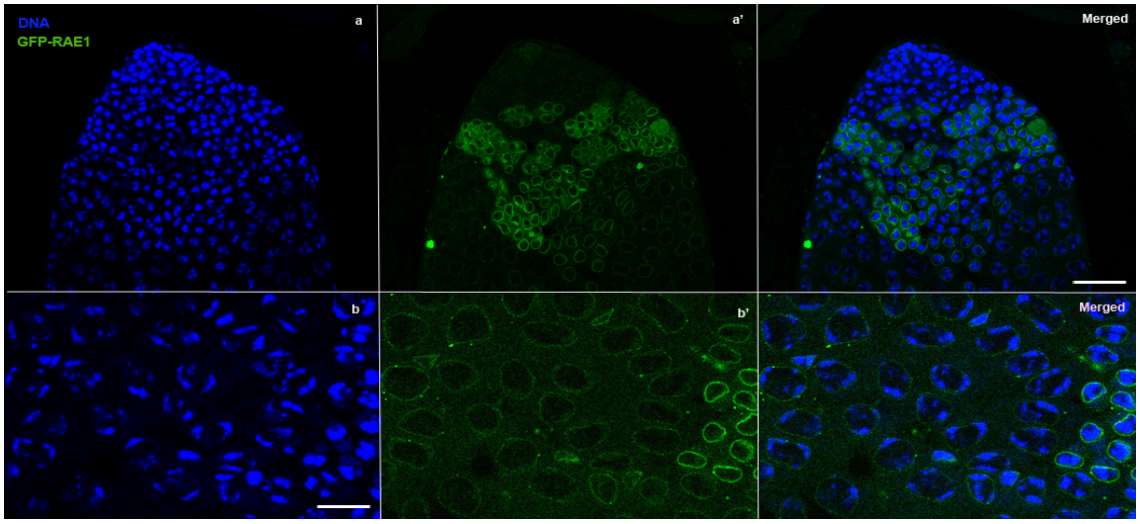

Figure 8. GFP-RAE1 localization pattern under the control of testis-specific GAL4 driver. DNA (DAPI staining) in blue, RAE1-GFP in green. (a) Testis apex. (a') The testis-specific BamGAL4 driver does not allow the expression of the GFP-RAE1 chimeric protein in the first stages of spermatogenesis. The cells at testis apex result avoid of GFP-RAE1 expression. The GFP-RAE1 signal appears at young polar spermatocytes showing a perinuclear and cytoplasmatic distribution. (b) Primary spermatocytes. (b')The GFP-RAE1 signal encircles the rim of nuclei. Scale bare 20 μn.

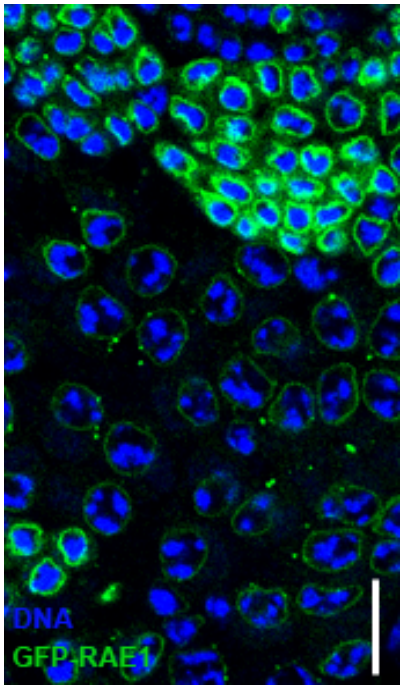

Figure 9. Particular of GFP-RAE1 localization pattern under the control of testis-specific GAL4 driver. DNA (DAPI staining) in blue, RAE1-GFP in green. Young (top) and late (bottom) spermatocyte stages. The GFP-RAE1 localized both with nuclear periphery and cytoplasm in young polar spermatocytes (top) and encircles the nuclear rim in primary spermatocytes (bottom). Scale bare 20 μn.

3.3.2 GFP-RAE1 localization under the control of *TubulinG4* driver

To overcome the temporal limits of of BamG4driver expression, I used a second ubiquitous driver, *TubulinG4*. In the early stages of spermatogenesis and in primary spermatocytes, the distribution of GFP-RAE1 was in accordance with that observed with the Bam driver. The chimeric protein localized at nuclear rim of the apex testis cells (Figure 10 a). The disintegration of Y loops defines the end of growth phase of primary spermatocytes and the beginning of meiotic phase (Cenci et al., 1994) At this stage, S6, chromatin begin to condense in preparation of meiotic division, the three chromatin clumps are still close to nuclear envelope but they start to congregate toward the center of the cells (Figure 10 b, DAPI staining). Notably, at this stage, the GFP-RAE1 signal not only still encircled the nuclei but resulted also associated with the chromatin clumps (Figure 10 b', GFP-RAE1 staining, arrowheads). During ana/telophase stages of first meiotic division, the two daughter nuclei appeared as compact chromatin masses (Figure 10 c, DAPI staining, arrows) separated by a central spindle where mitochondria localized. Note a DAPI staining halo of mitochondrial DNA colocalizing with the central spindle (Figure 10 c, DAPI staining, arrowheads). Significantly, the GFP-RAE1 signal localized with both newly formed nuclei and mitochondria at the central spindle (Figure 10 c', arrows for nuclei, arrowheads for central spindle).

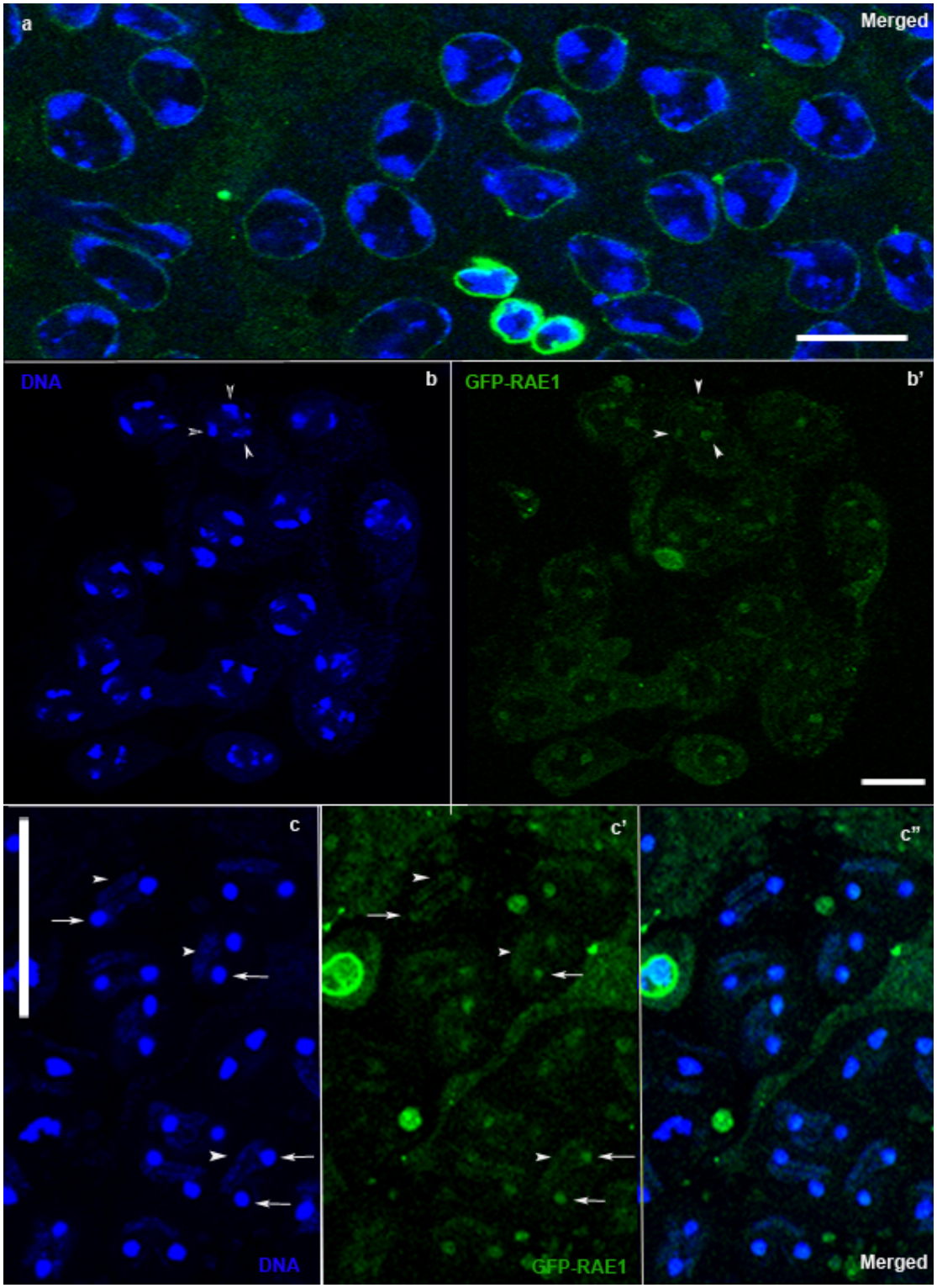

Figure 10. GFP-RAE1 localization pattern under the control of constitutive GAL4 driver. DNA (DAPI staining) in blue, RAE1-GFP in green. (a**)** Young Primary spermatocytes. The GFP-RAE1 signal shows a perinuclear distribution. (b) Late Primary Spermatocytes in meiotic prophase. The GFP-RAE1 signal still encircles the nuclei and localizes also with the three chromatin clumps (b' arrowheads). (c) Ana/telophase I cells. The RAE1-GFP signal colocalizes with the chromatin (c' arrows) and with mitochondria at central spindle (arrowheads). (C'') Merge of A and B. Scale bare 20 μn.

At the end of second meiotic division all haploid nuclei are associated with an organelle called Nebenkern formed by michondrial aggregates (Cenci et al., 1994) (Figure 11 top panel, DAPI staining, arrow for nuclei, arrowheads for Nebenkern). The GFP-RAE1 localized with Nebenkern, while nuclei are devoid of signal (Figure 11 top panel, GFP-RAE1 and merge, arrow for nuclei, arrowheads for Nebenkern). In mature sperms (Figure 11 bottom panel) the GFP-RAE1 signal marked both the heads and the tails of sperms (Figure 11 bottom panel, Merge).

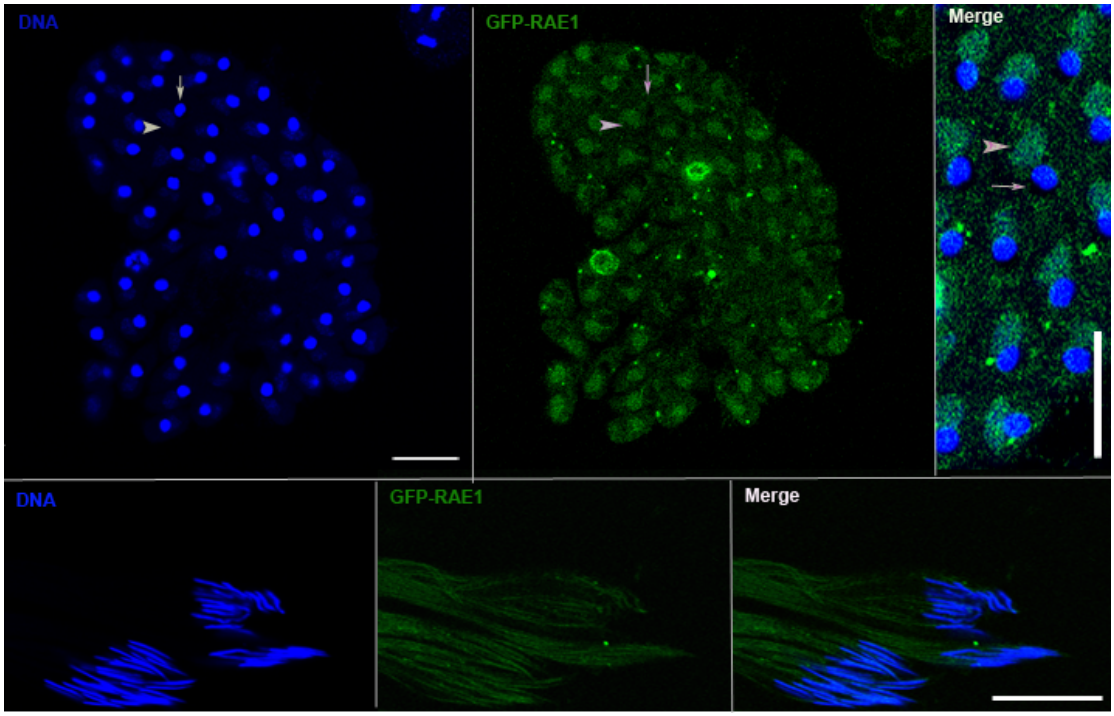

Figure 11. GFP-RAE1 localization pattern at post meiotic stages. DNA (DAPI staining) in blue, RAE1-GFP in green. (Top Panel). Each nucleus (DNA arrow) is associated with a Nebenkern (arrowhead). The RAE1-GFP signal localizes with Nebenkern (arrowhead in GFP-RAE1 and in Merged), and not with nucleus (arrow in GFP-RAE1 and in Merged,). (Bottom Panel) DNA in blue shows the heads of mature sperms. RAE1-GFP signal in green marks both heads and tails of mature sperms. Scale bare 20 μn

The pre-meiotic localization of GFP-RAE1 protein at nuclear envelope of early and late spermatocytes is in accordance with the previous observation in *S. cerevisiae* (Murphy et al., 1996) in mouse (HtTA line, Pritchard et al., 1999), in Drosophila (SL2 line, Sitterlin, 2004) and in human (HeLa line, Wong et al., 2006) culture cells. In the light of chromatin organization defects observed in *rae1* mutant flies in primary spermatocytes, the distribution at nuclear periphery could be linked with an involvement of RAE1 in meiotic chromatin condensation in preparation to meiotic divisions (Volpi et a., 2013). Moreover, the colocalization of GFP-RAE1 with chromatin from pro-metaphase up to

meiotic divisions and the presence of chromosmes fragmentation in both *ms(2)Z5584* mutant and *rae1* interfered males further support the connection between RAE1 and chromatin organization (Volpi et al., 2013). During meiotic divisions the GFP-RAE1 localized with both chromatin and central spindle mitochondria while once the meiotic phase is terminated at the onion stage, the protein moved to the Nebenkern leaving the nucleus completely devoid of signal. The presence of meiotic central spindle anomalies in *rae1* mutants and the association of GFP-RAE1 with central spindle mitochondria might be likely connected to a conserved role of RAE1 as interactor of proteins involved in spindle assembly in meiosis as in mitosis (Volpi et al., 2013). In this context it is noteworthy that the knockdown of Tpr nucleoporin results in the enhancement of chromosomes lagging due to an impaired recruitment of spindle checkpoint proteins to the dynein complex at kinetochore (Nakano et al., 2010). Notably, the fact that at the end of spermatogenesis the GFP-RAE1 protein was still present in heads and tails of mature sperms, indicates its involvement in spermatid differentiation. *rae1* mutant flies showed aberrant sperm head penotype that appeared round and unpolarized suggesting a RAE1 role in post meiotic chromatin condensation and organization as seen in pre-meiotic stages (Volpi et al., 2013).

3.4 The *GFP-rae1* transgene rescues the mutant phenotype of *ms(2)Z5584*

To verify if the chimeric GFP-RAE1 protein behavior recapitulated that of wild type protein, I checked if the transgenic construct *UAS-GFP-rae1* was able to rescue the sterile and cytological phenotype of $rae1^{Z5584}$ mutant males. To this aim, I conceived a complex experiment of five successive crosses to generate $rae1^{Z5584}$ homozygous flies carrying the *Tubulin* GAL4 driver and the *UAS-GFP-rae1* construct in transheterozygosity on the 3rd chromosome (Figure 12). I found that the GFP-RAE1 chimeric protein was able to fully rescue the $rae1^{Z5584}$ sterile phenotype. Rescued fertile males were cytologically tested to check if the cytological defects of *ms(2)Z5584* were also rescued. Primary spermatocytes of rescued males showed a normal organization of chromatin with the GFP-RAE1 signal localized at nuclear periphery as in wild type (Figure 13 a, a'). Rescued spermatids at onion stage showed a normal 1:1 ratio of nuclei and Nebenkern that appeared of identical size (Figure 13 b, b'). Moreover, at that stage the distribution of GFP-RAE1 chimeric protein is identical to wild type (not shown). These results confirm definitely that the cytological defects characterizing *ms(2)Z5584* mutants were also completely restored by the *GFP-rae1* construct expression.

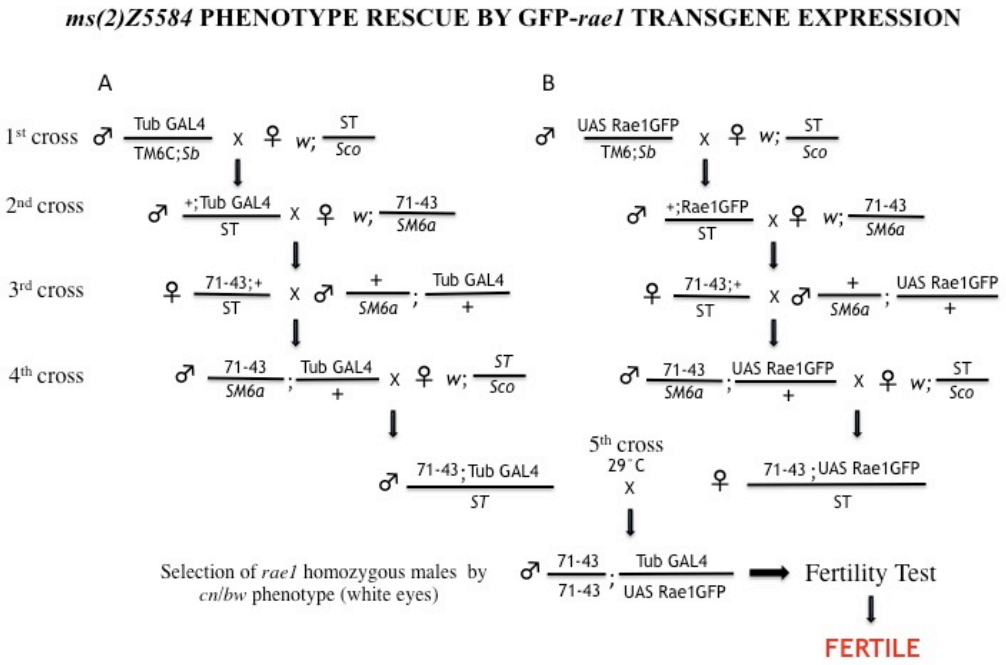

Figure 12. Rescue experiment: outline of crosses. The 71-43 line carries in homozygosity a second chromosome bearing both the *rae1*^{Z5584} mutation and the *cn*, *bw* markers. A *rae1*^{Z5584} homozygous flies carrying both the *Tubulin* GAL4 driver and the *UAS Rae1-GFP* construct on the 3rd chromosome were generated at the 5th crosse and selected by homozygous *cn/bw* white eye phenotype. These flies were tested for fertility and the cytological phenotype was tested. The fertility was tested in a mating with *yw* vergin female. The GFP-RAE1 chimeric protein was fully able to rescue all the *rae1*^{Z5584} phenotypes.

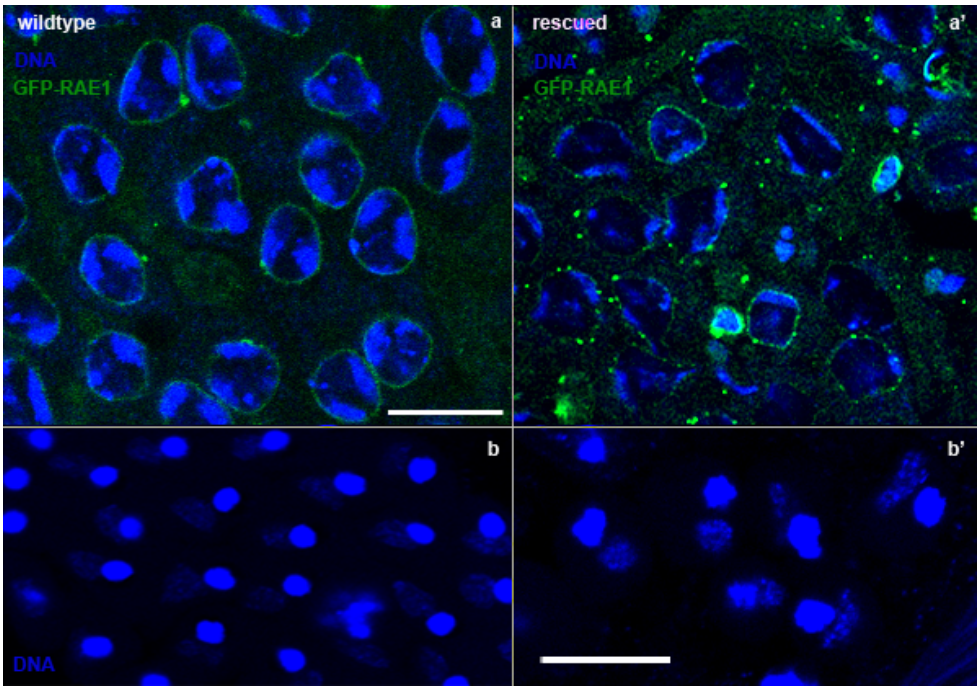

Figure 13. Cytology of rescued males. DNA (DAPI staining) in blue, RAE1-GFP in green. (a) Wild Type young primary spermatocytes show a perinuclear distribution of GFP-RAE1. (a') Young primary spermatocytes of rescued males exhibit a wild type chromatin phenotype and the RAE1-GFP signal shows a perinuclear distribution as in wild type. (b) Wild type onion stage. (b') Spermatids at onion stage of rescued males, the shape and the 1:1 ratio between nuclei and Nebenkern is normal. Scale bare 20 μn.

Notably, the GFP-RAE1 transgene was also able to rescue post-meiotic $rae1^{Z5584}/rae1^{Z5584}$ mutant phenotypes up to mature sperms. Mutant mature sperms showed aberrant nuclear morphology that resulted in round and unpolarized heads (Figure 14 a), suggesting that chromatin condensation events and sperm individulization process are heavily compromised. Mature sperms of rescued males appeared completely normal, with needle-shaped and polarized heads (Figure 14 b).

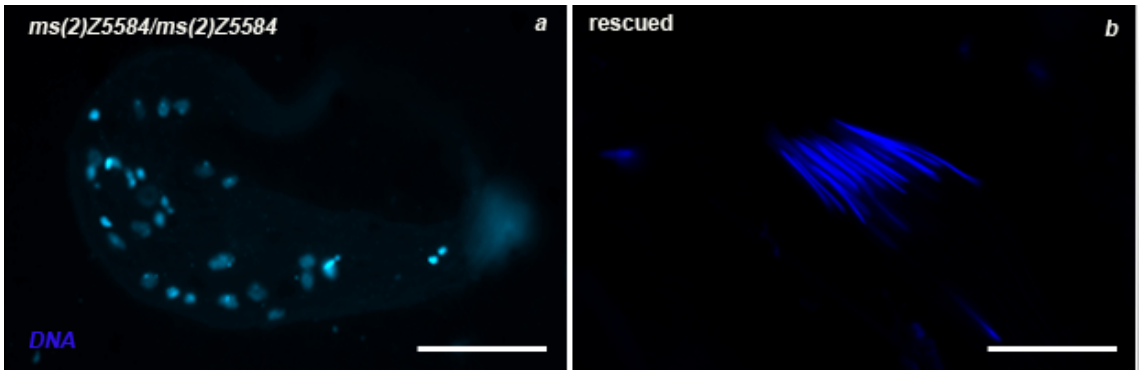

Figure 14. Cytology of mature sperms in rescued males. DNA (DAPI staining) in blue. (a) $rae1^{Z5584}/rae1^{Z5584}$ homozygous mutant males show unpolarized sperm heads with round uncondensed nuclei. (b) RAE1-GFP chimeric protein is able to rescue mutant phenotype up to post-meiotic differentiation stages producing normal sperms and restoring fertility. Scale bare 20 μn.

Thus, the GFP-RAE1 chimeric construct was able to fully rescue the sterility and cytological phenotypes of $rae1^{Z5584}/rae1^{Z5584}$ mutants, implying that it can mimic the wild type protein behavior. This evidence means that the RAE1 protein localization pattern inferred by the *UAS-GFP-rae1* transgene is definitely comparable to the wild type one.

In conclusion, both the *rae1* RNAi experiments and the entire phenotype rescue by the chimeric construct, fully confirmed that *rae1* is the gene responsible of phenotypes observed in *ms(2)Z5584/ ms(2)Z5584* mutant strain. My results strongly demonstrate that *RAE1* have a fundamental and unexpected role in the execution of proper meiosis and spermatogenesis.

3.5 *ms(2)Z1168* mutant strain: starting point

The *ms(2)Z1168* mutant strain is a member of the collection of 13 EMS-induced male sterile recessive mutants on chromosomes 2 and 3 (Wakimoto et al., 2004). By recombination and complementation mapping, the cytological region harboring the mutation was restricted to the interval 29A3-29B1 on the left arm of chromosome 2. *ms(2)Z1168* belongs to *twine* class as it skips both meiotic divisions but post-meiotic differentiation stages take place; however, a genetic characterization of *ms(2)Z1168* mutant excluded a possible allelism with *twine*. *ms(2)Z1168 in vivo* cytology highlighted nuclear blebbing phenotype in primary spermatocytes (Figure 15 a) , aberrant onion stage characterized by a giant mitochondrial aggregates and small or undetectable nuclei due to extreme chromatin fragmentation (see below) (Figure 15 c). The formation of mature, although defectives, sperms still takes place. Chromatin staining highlighted condensation defects both in primary spermatocytes (Figure 15 b) and in onion stages where diploid spermatids presented a higly decondensed chromatin (Figure 15 c'). Preliminary results showed that in *ms(2)Z1168* mutant males the nuclear lamina was compromised. When working to the cytological characterization of nuclear lamina in *ms(2)Z1168* mutant males, I realized that the wild type nuclear lamina characterization during the process of meiosis and spermatogenesis was missing in literature. Here, a complete description of nuclear lamina in wild type and in *ms(2)Z1168* mutant is reported.

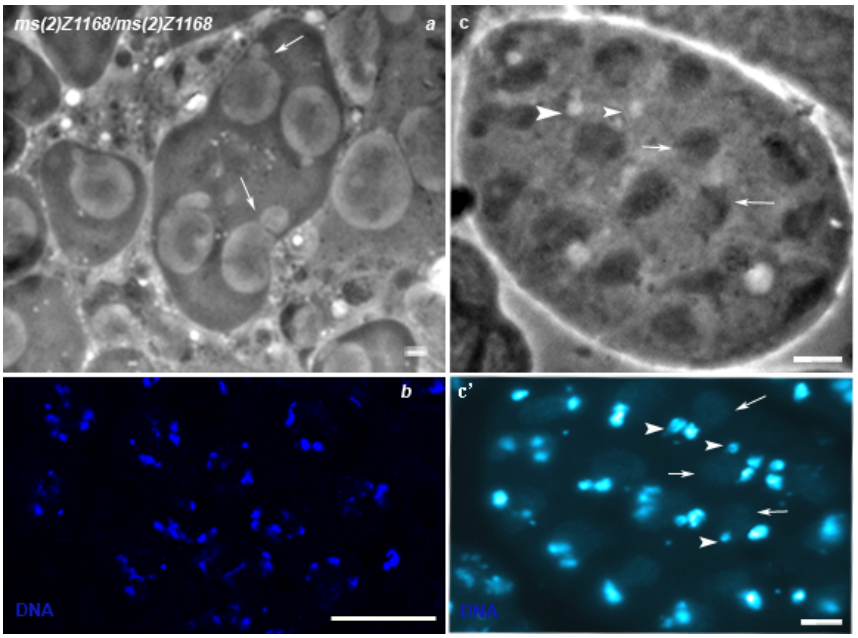

Figure 15 In vivo and fixed cytological analysis of ms(2)Z1168. Nuclear blebbing in primary spermatocytes (a, *in vivo*, arrows). Chromatin condensation defects in primary spermatocytes (b, DAPI staining). The same spermatids cyst *in vivo* (c) and fixed (c'). Giant mitochondrial aggregation at onion stage (c and c', arrows) associated with small nuclei (c and c', arrowheads). Note that Nebenkern associated chromatin is visible only at DAPI staining (c') and not at phase contrast (c) due to the high degree of chromatin decondensation. Scale bar 20 μm.

3.6 Nuclear lamina localization during pre-meiotic stages in the wild type

For the characterization of nuclear lamina localization pattern throughout spermatogenesis, we immunostained fixed testes with a primary antibody anti-laminDm0, the major component of the Drosophila lamina. In spermatogonial cells, the nuclear lamina appears as a continuous, sharp signal surrounding the nucleus (not shown), which is identical to that of young primary spermatocytes . In young primary spermatocytes at prophase (S3 stage, staging refers to Cenci et al., 1994) when chromatin was divided in three distinct masses corresponding to the three major bivalents (Figure 16 a, DAPI staining), the nuclear lamina appeared as a thick signal uniformly distributed at nuclei periphery (Figure 16 a, anti Lam-Dm0). In primary spermatocytes at S4 stage, which were recognizable because of their larger nuclear size as compared to young spermatocytes (Figure 16 b), the nuclear lamina showed a signal comparable to that seen in the preceding stage (Figure 16 b, anti Lam-Dm0 in green). Instead, the lamina signal became irregularly shaped and invaginations became apparent in mature spermatocytes at S5 stage (Figure 16 c, arrows) when the three chromatin clumps reached their maximum size (Figure 16 c, DAPI staining in red).

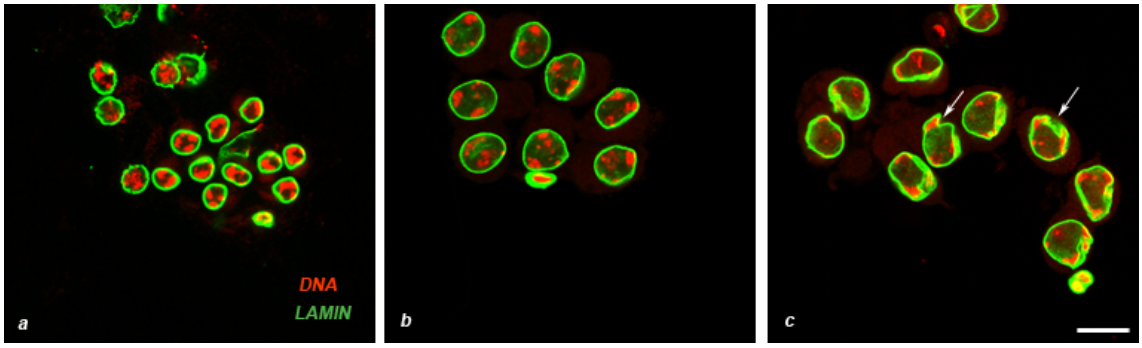

Figure 16 Nuclear lamina behavior in meiotic prophase cells. DNA in red (DAPI staining), Nuclear lamina in green (anti Lam-Dm0). In young primary spermatocytes at S3 stage (a) and primary spermatocytes at S4 stage (b) the lamina signal uniformly encircles the nuclear rim. In mature primary spermatocytes at S5 stage (c) the nuclear lamina shows an irregular shape and invaginations (arrows). Scale bar 20 μm.

These observations are consistent with previous evidences in drosophila embryos and in mammalian culture cells. In drosophila, early embryo mitotic interphase nuclei show a continous nuclear lamina structure at their periphery (Harel et al., 1989), changes in the nuclear envelope structure appear during the between late prophase to metaphase transition (Fuchs et al., 1983; Hiraoka et al., 1990a; Paddy et al., 1990), when invaginations of nuclear lamina are visible in a regions close to centrosomes thus suggesting an interaction between centrosomes and lamins (Paddy et al., 1996). In mammalian cells during G2/M transition the progressive chromosome condensation is coupled with invaginations in nuclear lamina leading to a distortion of the entire structure by microtubules mechanical tension (Beauduin et al., 2002).

3.6.1 Nuclear lamina behavior during meiotic divisions in the wild type

Prometaphase nuclei at M1b stage were characterized by the equatorial alignment of the three highly condensed chromatin masses (Figure 17 a and b, arrows). At this stage the nuclear envelope broke down and the nuclear lamina signal appeared discontinuous (Figure 17 a'and b', arrowheads). In mammalian mitotic cells, following prophase invaginations, nucleus becomes permeabilized and gaps in the nuclear envelope structure appear in association with chromosomes congression (Beauduin et al., 2002). Due to a correlation between centrosomes migration and nuclear lamina deformation in mitosis of early Drosophila embryo (Paddy et al., 1996) and between spindle microtubules and nuclear envelope invaginations in mammalian cells (Beauduin et al., 2001), we can likewise speculate a possible correlation between centrosomes, meiotic spindle formation and nuclear lamina structure deformations during meiotic prometaphase of Drosophila male meiosis. In metaphase I, bivalents congregated and appeared as a compact, single chromatin mass (Figure 17 c, Stage M3). The nuclear lamina still surrounded the condensed chromatin but the signal was diffused and not well structured as in the previous stage (Figure 17 c' and c"). This is consistent with early observations in rat culture cells (Gerace et al., 1978). This diffused pattern is supposedly associated with depolymerization of nuclear lamina structure. Phosphorylation of lamins at particular positions mediates the disassembly mechanism of nuclear lamina during mitosis (for a review see Dechat et al., 2010). Higher magnification of late anaphase I (Figure 17 d, Stage M4c) and telophase I (figure 17 e, Stage M5) showed that the nuclear lamina signal surrounded the nuclei with a thick,

irregularly shaped design (Figure 17 d', d'' and 17 e', e", respectively) that thus differed from the thin, circular signal of premeiotic stages. Moreover, at these stages, the nuclear lamina showed also a punctuate signal associated to the mitochondria of the central meiotic spindle (Figure 17 d", e" arrows). The sequence of these events appears different from that observed in Drosophila embryo mitotic cells in which the lamina signal results well localized as a rim at nuclear periphery up to the metaphase and the lamin delocalization process is completed only when chromosomes moves to anaphase (Paddy et al., 1996). Second meiotic division advanced very quickly and the nuclear lamin pattern showed the same pattern observed during the first meiotic division. The nuclear lamina appeared as a diffuse signal at metaphase II (figure 17 f, merge), and it reassembled at the periphery of daughter nuclei in anaphase II (Figure 17 g) and telophase II nuclei (Figure 17 h). However, the signal encircling the nuclei appeared thicker than in the same stages of the first division. A well-structured assembled lamina during meiotic division seems to be a mandatory condition to ensure a correct chromosomes segregation during male meiosis. Interference of *lmn-1* gene implies defects in chromatin condensation and chromosomes segregation in *Caenorhabditis elegans* (Liu et al., 2000). In mammalian cells Lamin B is associated with chromosomes during congression to metaphase (Georgatos et al., 1997). In Drosophila somatic cells evidences indicate that the nuclear lamin is directly connect with chromatin. Lamins proteins bind the histone core *in vitro* (Taniura et al. 1995) and specific DNA sequences called matrix attachment regions (Luderus et al., 1992). More, Lamin Dm1 and Lamin Dm2 bind *in vivo* nucleic acids, the H3- H4 histone tetramer, the mitotic chromosomes and the heterochromatin protein HP1. Furthermore electron microscopy studies show that some areas of chromatin are in close contact with the nuclear lamina (Paddy et al., 1990). In *D. melanogaster* specific chromosomal regions are associated with nuclear envelope and some evidence suggests that these regions are inactive chromatin (Mathog and Sedat, 1989). Recently, it has been proposed a model of nuclear architecture in which lamins position the chromosomes in the nucleus (Reddy et al. , 2008).

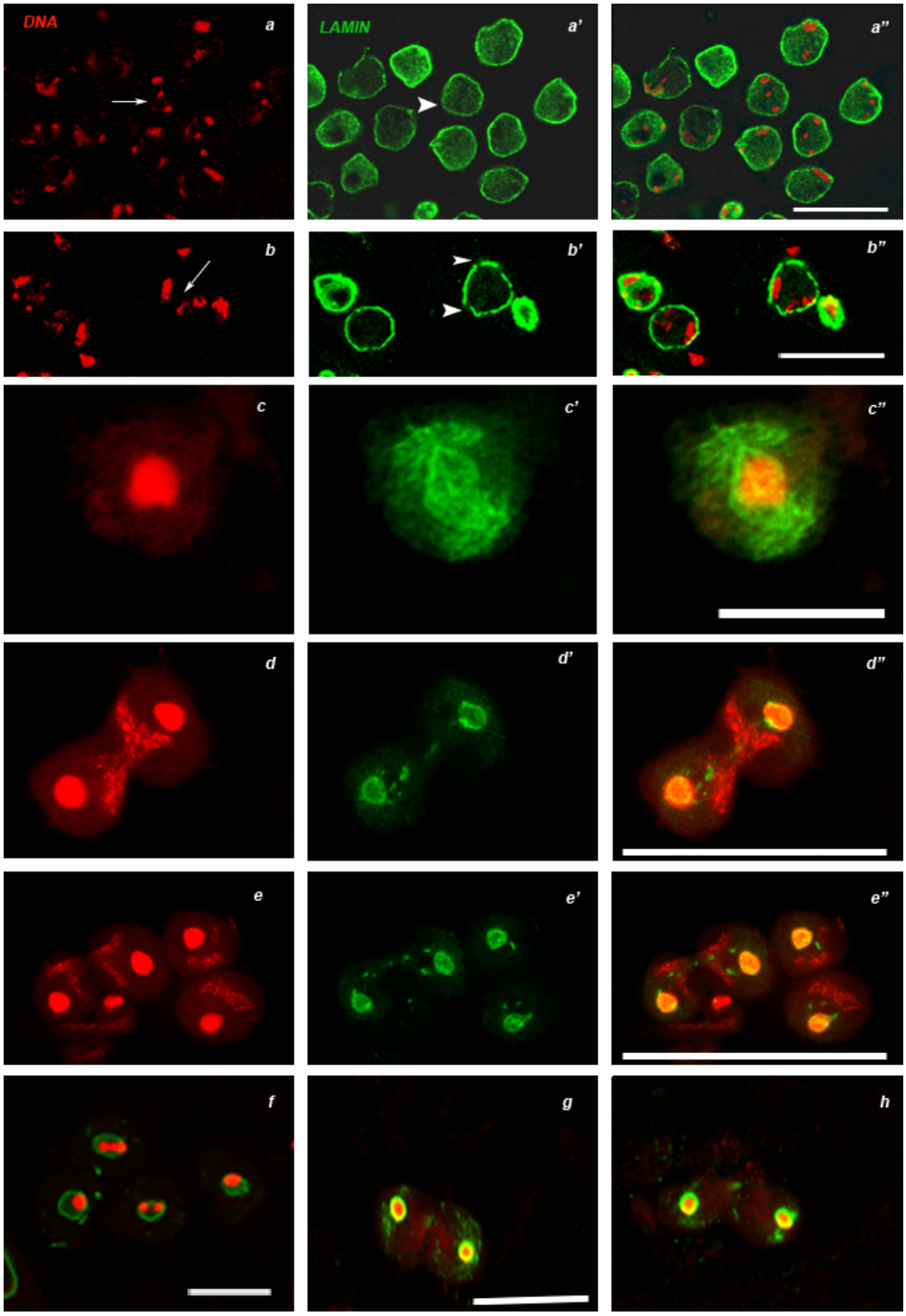

Figure 17 Nuclear lamina pattern during prometaphase and meiotic divisions. DNA in red (DAPI staining), Nuclear lamina in green (anti Lam-Dm0). In prometaphase cells at M1b stage, the three chromatin clumps corresponding to the three major bivalents (a and b, arrows) move to the equatorial plate, the nuclear envelope breaks down and the lamina signal becomes discontinous (a' and b', arrowheads). In metaphase I, nuclei (stage M3) appear as a single condensed chromatin mass (c), the nuclear lamina signal appears diffused in the nucleoplasm (c'). Anaphase (d) and telophase (e) nuclei, the reformed nuclear lamina exhibits a thick, irregularly shaped signal. Note the punctuated nuclear lamina signals which are associated to the central spindle identified by the typical hourglass configuration of mitochondria. In Metaphases II nuclei at M2 and M3 stages, nuclear lamina appears as diffuse signal around chromatin (f). In anaphase II (g) and telophase II (h), nuclear lamina shows a well-defined structure at daughter nuclei periphery. Scale bar 20 μm.

3.6.2 Nuclear lamina localization pattern in post-meiotic stages of spermatogenesis in the wild type

The result of the two meiotic divisions is the formation of a 64 haploid spermatid cyst. At the end of telophase II, mitochondria aggregated forming first an irregular mass of variable shape associated with the nucleus (Figure 18 a, Stages T1 and T2, arrows). At that stage, nuclear Lamina showed a punctuate pattern at the nuclear rim (Figure 18 a' and a"). With the progress of spermatid differentiation, at onion stage (Figure 18 b, Stage T3), the thick nuclear lamina signal encircling the nucleus showed interruptions (Figure 18 b', arrowheads). At T5 stage, when spermatid chromatin underwent decondensation and Nebenkern assumed an oval shape (Figure 18 c, arrows), the nuclear lamina signal appeared not only at the rim but also inside the nuclei (Figure 18 c', and c"). During spermatid elongation process, chromatin condensed again, and Nebenkern elongated forming the primordium of the future sperm tail (Figure 19 a and b, arrows). At that stage, the nuclear lamina signal dramatically changed becoming localized only at the side of the nucleus from which the tail lengthened thus assuming a "half moon" configuration (Figure 19 a', a", b', b" arrows). The spermatogenesis process culminates in the differentiation and maturation of sperms, (Figure 20, DAPI staining). The mature sperms heads were completely devoid of nuclear lamina signal (Figure 20, Lam-Dm0). The correlation between chromatin and nuclear lamina behavior seems thus to accompany also the post-meiotic stages of spermatogenesis. The apparent ability of the nuclear lamina to reorganize in relationship with chromatin condensation emphasizes again its great dynamism. The observed pattern is in accordance with the functions of nuclear lamina in determining and maintaining the nuclear shape. In fact, the condensation/decondensation events imply nuclear conformational changes that may be likely supported by nuclear lamina reorganization. Moreover, the differences in the composition of nuclear lamina of spermatogenetic cells with respect to the somatic counterpart were proposed to be connected to the need of modulating nuclear organization changes during spermatogenesis. The fact that mammals germ line lamins B3 and C2 are shorter and in minor amounts with respect to the somatic lamins, would lead to the formation of a more flexible lamin structure and therefore more suited to address nuclear changes characterizing gametogenesis (For a review see Schutz et al., 2005).

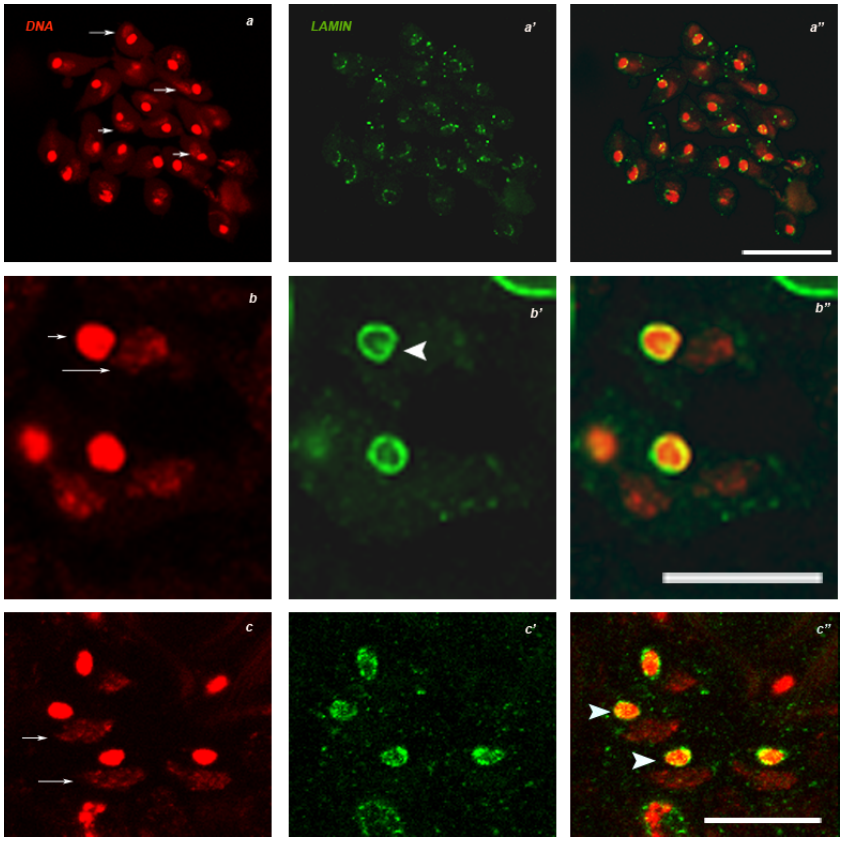

Figure 18 Nuclear lamina distribution during spermatids differentiation. DNA in red (DAPI staining), Nuclear lamina in green (anti Lam-Dm0). T1 and T2 stages are characterized by the progressive aggregation of mitochondria into masses of different shapes (a, arrows). Nuclear lamina exhibits a punctuate pattern at the nuclear rim (a'). At onion stage nucleus and Nebenkern in a 1:1 ratio (b, short and long arrows, respectively) have the same round shape and size. Nuclear lamina shows a thick appearance at nuclear periphery, with interruptions (b', arrowhead). T5 spermatids stage are characterized by an oval shaped Nebenkern (c, arrows) with the nuclear lamina signal localized over the nuclei (c', arrowheads). Scale bar 20 μm.

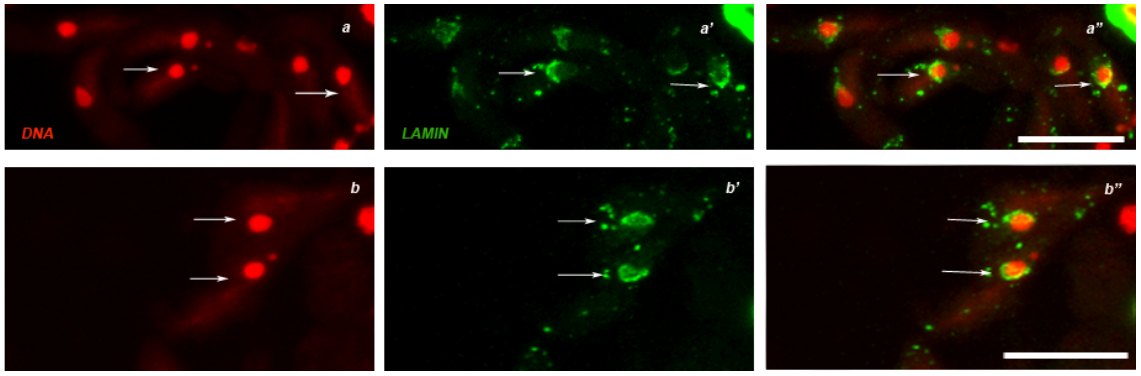

Figure 19 Nuclear lamina distribution during the spermatid elongation process. DNA in red (DAPI staining), Nuclear lamina in green (anti Lam-Dm0). Note the "half moon" configuration of nuclear lamina (a', b', a", b") that localizes at one nucleus side coinciding with the elongating Nebenkern (a and b, arrows). Scale bar 20 μm.

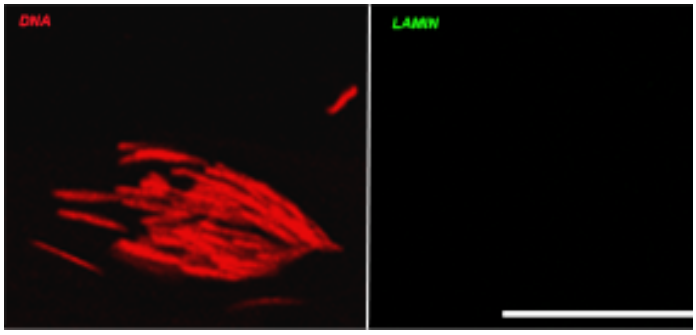

Figure 20 Nuclear lamina in mature sperms. DNA in red (DAPI staining), Nuclear lamina in green (anti Lam-Dm0). The nuclear lamin signal is completely absent from both the needle-shaped sperm heads and the tails. Scale bar 20 μm.

With the progress of spermatids elongation, we observed an enrichment of nuclear lamina at one side of nucleus where the spermatids tail extends. During mammalian spermiogenesis lamins show different distribution pattern: lamin C2 is expressed in meiotic stages (Alsheimer and Benevante, 1996) and lamin B3 in later stages of spermatogenesis (Shutz et al., 2005), whereas lamin B1 is the only isoform always detectable throughout the whole process (Vester et al., 1993). Notably, during mouse spermiogenesis lamin B3 polarized at the posterior pole of elongated spermatid nuclei (Shutz et al., 2005), a localization fully comparable to the one we observed in flies, suggesting a polarized pattern for lamin proteins at the final stage of spermatogenesis which is conserved between species. In mammalian post meiotic stages, several nuclear envelope associated proteins polarized and resulted undetectable in differentiated mature sperm (Alsheimer et al., 1998). This behavior was observed for proteins that directly or indirectly interact with chromatin as lamin B1 (Vester et al., 1993), LAPs2 (Alsheimer et al., 1998), germ cell-less (GCL) (Kimura et al., 2003), and lamin B receptor (LBR) (Mylonis et al., 2004). It is possible that the redistribution of nuclear envelope proteins to the posterior pole of spermatids, the only site where chromatin is attached, would contribute to the achievement of chromatin distribution in the sperm (Alsheimer et al., 1998). The overview emerging from that characterization is a continuous structural change in the structure of the nuclear lamina from meiotic prophase until the end of spermatogenesis. These structural changes seem to parallel the process of condensation/decondensation of chromatin throughout the process. Our observation are in line with the pioneering immunofluorescence data describing changes of nuclear lamina distribution throughout the mitotic cell cycle (Gerace and Blobel, 1980; Gerace et al., 1978) thus reinforcing the general idea of the prominent role of nuclear lamina in modulating the dynamics of the nuclear membrane architecture.

3. 7 *ms(2)Z1168* homozygous mutant males show defects in nuclear lamina structure

In *ms(2)Z1168* homozygous mutant young polar spermatocyte at S2a stage the chromatin appeared as unique and compact mass (Figure 21 a, DAPI staining in red, arrow), then progressing to the S2b stage chromatin became divided in three clumps (Figure 21 a, DAPI staining in red, arrowhead) as in wild type. The nuclear lamina signal appeared continuous but not circular as in wild type (Figure 21 a', anti Lam-Dm0 in green). Progressing with the spermatocyte development, the mutant chromatin pattern is so severely compromised that it is difficult to distinguish the different stages of spermatocyte development. The three chromatin clumps observed in young spermatocytes were no longer visible in mature primary spermatocytes where instead chromatin appeared highly disorganized (Figure 21 b, DAPI staining in red) and nuclear lamina assumed irregular shapes (Figure 21 b', anti Lam-Dm0 in green) where wild type invaginations could never be observed. In rare prometaphase I nuclei (Figure 21 b, arrow) the nuclear lamina showed an irregular shape, devoid of wild type openings and the lamina breakdown did not apparently occur (Figure 21 b, anti Lam-Dm0 in green, arrow). Taken together these data indicate that in the mutant aberrations of nuclear lamina and chromatin condensation defects concomitantly occurr leading to the alteration of meiotic cell cycle progression. The second chromosome cytological region harboring the *ms(2)Z1168* mutation (29A3-29B1) contains 12 genes, none of which encodes for lamin proteins. It is plausible to hypothesize that the observed irregular lamin phenotype in an *ms(2)Z1168* mutant flies may not be attributed to a mutation of lamin encoding genes but of genes expressing nuclear envelope associated proteins necessary for proper lamina organization and behavior. For example, in mouse the *mgcl-1* gene, a mouse homolog of Drosophila melanogaster *gcl* gene, encodes for a protein mGCL-1 that binds LAP2β, an inner nuclear membrane protein interacting with lamin B and chromosomes (Foisner and Gerace; 1993). mGCL-1 null mice show reduction of fertility, meiotic nuclear morphology defects, and chromatin condensation defects associated with a defective expression of transition proteins and protamines during spermatogenesis (Kimura et al., 2003). Notably, in Drosophila early embryos the nuclear lamina invaginations were observed in the regions immediately close to the centrosomes, and authors suggest a connection between centrosomes migration and nuclear lamina behaviour (Paddy et al., 1996). In the light of these findings and considering the absence of functional centrosomes and the presence of nuclear lamina

defects in *ms(2)Z1168* mutant flies, I can speculate that the gene at the basis of mutant phenotypes, could encode for a protein involved in the interaction between centrosomes and nuclear lamina and that the lack of this interaction in the mutant precludes the organization of functional centrosomes.

Moreover, due to the complexity of nuclear lamina network, it is plausible to speculate that the observed aberrant phenotype characterizing the mutant might be associated to anomalies during nuclear lamina assembly/disassembly process or in maturation events that involves pre-lamin proteins.

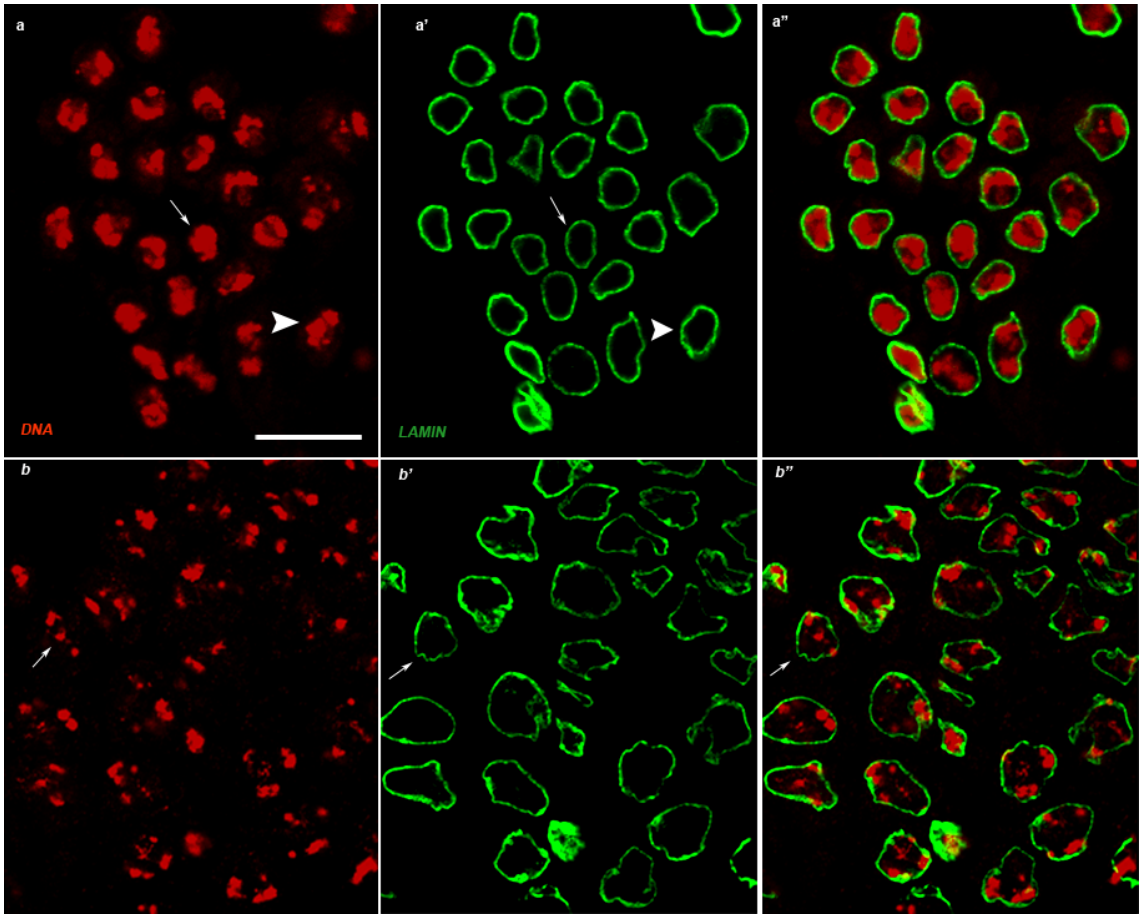

Figure 21 Pattern of nuclear lamina in a male meiotic mutant. DNA in red (DAPI staining), Nuclear lamina in green (anti Lam-Dm0). In young primary spermatocytes at S2a/S2b stage (a, DAPI staining in red, arrow: primary spermatocytes nucleus at S2a stage, arrowhead: primary spermatocytes nucleus at S2b stage) the lamina signal uniformly encircles the nuclear rim as in wild type (a', anti Lam-Dm0 in green) At late spermatocyte and prometaphase stages (b, arrow points to a prometaphase nucleus) the chromatin shows condensation defects, whereas the nuclear lamina assumes irregular shapes and the breakdown does not occur (b', anti Lam-Dm0 in green). Scale bar 20 μm.

3.8 Towards *ms(2)Z1168* gene identification

Meiotic recombination mapping, performed by a strain carrying phenotypic recessive markers on chromosome 2, allowed to map the *ms(2)Z1168* mutation around 37.4 m.u within the interval *dp-b*. By deficiency mapping, the genetic region containing the mutation was further restricted up to the cytological interval 29A3-29B1 (Figure 22). The region contains 12 genes: CG7818, CG7810, CG7806, CG7795 (*mtsh*), CG7787, CG7781, CG14275, CG14274, CG14273, CG7778, Mur29B, CG7627.

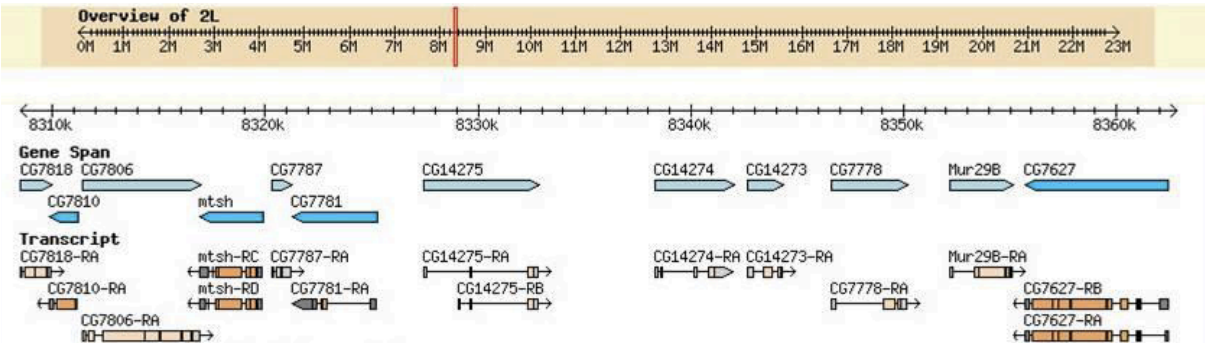

Figure 22. 29A3-29B1 chromosome 2 region. The region is 54 Kbp, from 8308491bp to 8362842bp.

To identify the mutated gene in the *ms(2)Z1168* strain, I first followed a reverse genetic approach using the RNA interference technique and, second, a molecular approach by gene sequencing. As previously described (see paragraph 3.2), I first selectively knocked down six of the twelve genes chosen on the basis of their high expression in the testis, by the GAL4/UAS system using the testis-specific driver *BamG4UASDicer2* (see scheme in paragraph 3.2, figure 6). I tested the interfered males for fertility and compared the induced-RNAi phenotype with that observed in *ms(2)Z1168* mutant. The results of fertility test for each interfered gene are reported in the following table.

SILENCED GENE	FERTILITY TEST
CG7627	FERTILE
CG7778	FERTILE
CG7787	FERTILE
CG7810	**STERILE**
CG7818	FERTILE
CG7806	FERTILE
CG7795 (mtsh)	**STERILE**

Results of fertility test in interfered males. The genes reported in the table were silenced by RNAi driven by a testes-specif driver. *CG7810* and *CG7795* resulted sterile in a cross with vergin *yw* females.

Of gene silenced, *CG7810* and *CG7795* knockdown male flies resulted sterile. *CG7795*, *mitoshell* (*mtsh*), encodes a bromodomain-related protein and *mtsh* mutant males are sterile, with pre-meiotic premature mitochondrial aggregation that produces a shell surrounding spermatocyte nuclei. *mtsh* mutant spermatocytes perform meiotic divisions resulting in four nuclei associated with a single mitochondrial shell at onion stage (Bergner et al., 2010). Since the *ms(2)Z1168* homozygous mutant phenotype resulted quite different from that of *mitoshell* knockdown flies, I could exclude that the mutated gene responsible for the mutant phenotype of *ms(2)Z1168* strain was *CG7795*. A complementation test between the chromosome *ms(2)Z1168* and a *mtsh* allele will be necessary to further support the phenotypic differences. *CG7810* is a yet uncharacterized gene, that encodes for a coiled-coil domain containing protein with unknown function (FlyBase.org). *In vivo* cytology of *CG7810* RNAi males showed herniations in primary spermatocytes very similar to those observed in *ms(2)Z1168* homozygous mutant males (Figure 23). On the contrary, onion stage spermatids showed aberrant Nebenkern structure of variable size and non-spherical shape that differed from the onion stage aberrant phenotype of *ms(2)Z1168* homozygous mutant males (Figure 24). This discrepancy might be likely caused by the limited window of interference due to the absence of *BamG4UASDicer2* driver expression in post-meiotic stages.

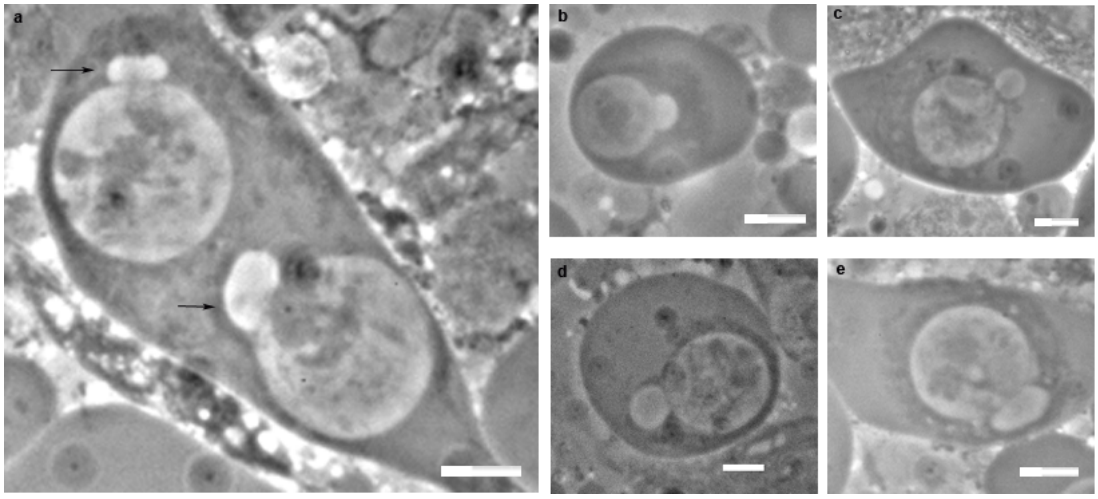

Figure 23 *CG7810* dsRNA induces aberrant phenotypes in primary spermatocytes. (a, b, c, d, e) Primary spermatocytes of *CG7810* dsRNA males showing nuclear herniations comparable with that observed in *ms(2)Z1168* homozygous mutant males (compare with Figure 11a). Scale bar 20 μm.

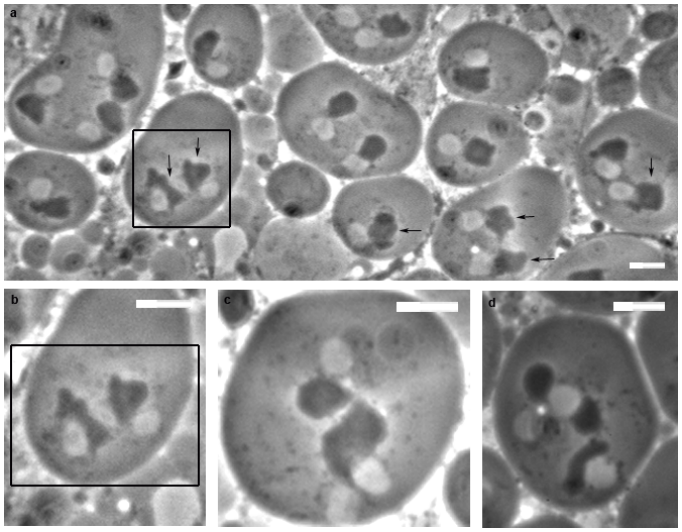

Figure 24 *CG7810* dsRNA induces aberrant phenotypes in onion stage spermatids. (a) Spermatids at onion stage show anomalies in Nebenkern which result irregular both in shape and size (arrows). (b) Magnifiction of the selected area of panel a. (c and d) Magnification of other Nebenkern aberrations. The CG7810 phenotype induced by RNAi results different from that observed in *ms(2)Z1168* homozygous mutant males (compare with Figure 11b). Scale bar 20 μm.

Under the light of those phenotypic evidences, *CG7810* seems to be a reasonable candidate gene underpinning the mutant phenotype of *ms(2)Z1168* strain. A molecular approach by gene sequencing was used to verify the possible presence of a mutation in *CG7810*.

3.8.1 *CG7810* sequencing

Genomic DNA was extracted in the *ms(2)Z1168* homozygous flies, the *CG7810* gene was amplified by specific primers and PCR products were sequenced (see 5.8 chapter in Material and Methods). The *CG7810* sequences from *ms(2)Z1168* homozygous flies were compared to the *CG7810* sequence from the *D. melanogaster* genome sequence, (release number: FB2014_02 - March 14th). Moreover, to exclude that the mutation was already present in the strain used for mutagenesis, I sequenced and used for further comparison the *CG7810* gene from another mutant belonging to the original Zucker collection. The analysis of sequences evidenced three adjacent mutations consisting in two point mutations, from T to A and from C to A, and a deletion of one nucleotide. These three mutations reside 77bp upstream of the 5'UTR (bases locations: 2L: 8,311,277/278/279), within an intergenic region of 203bp between *CG7810* and *CG7806* genes (Figure 25).

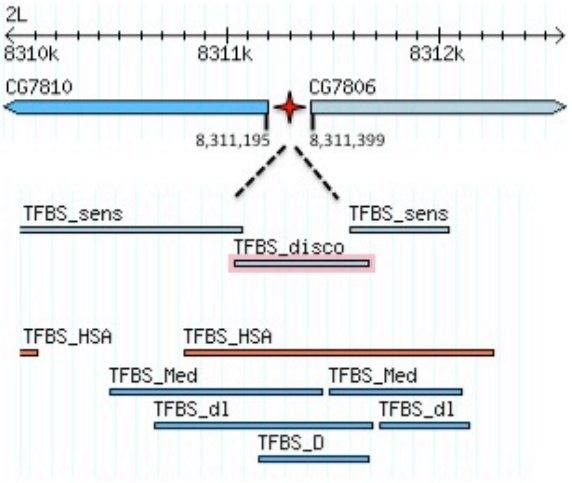

Figure 25. Genomic region of *ms(2)Z1168* mutations. Mutations reside in a intergenic region between *CG7810* and *CG7806* (red star). The genomic region from 5' UTR of *CG7810* (location 8,311,195) to 5' UTR of *CG7806* (location 8,311,399) is 203bp long and has been identified as trascription factors binding site. In bottom part of the scheme the Trascription Factors (TFBS) that bind the region are reported.

The 230bp sequence was reported as Transcription Factor binding site by HOT Spot analysis (HSA) (*The modENCODE Consortium, 2010*). Several transcription factors able to bind the region were identified by ChIP-Seq analysis (*The modENCODE Consortium, 2010*): TFBS_disco, TFBS_Med, TFBS_dl and TFBS_D. In particular, TFBS_disco and TFBS_D exactly bind the intergenic region between *CG7810* and *CG7806* and both show a positive transcription regulation activity. Although till now neither seem to be directly involved in the process of spermatogenesis, nevertheless

both, especially TFBS_D, are expressed in testis. In the light of these evidences, it is reasonable to speculate that the mutations in the sequence of TF binding site can influence the binding of one or more transcription factors leading to a failure of gene transcription. Due to the proximity to *CG7810* gene, we can speculate that the 230bp sequence may constitute the promoter of the gene. It is interesting to note that a canonical TATA box element is not present in the sequence at 5' of the *CG7810* gene. With exceptions, the TATA-containing or TATA–less promoters could discriminate between housekeeping and tissue-specific genes (Arkhipova, 1994), thus reinforcing the idea that the *CG7810* gene had a tissue-specific function, possibly in spermatogenesis.

4. CONCLUSION AND FUTURE PERSPECTIVES

In the present work, I analyzed two Drosophila melanogaster mutant strains, *ms(2)Z5584* and *ms(2)Z1168,* belonging to a unique collection of 13 EMS-induced male sterile recessive mutations on chromosome 2 (Wakimoto et al., 2004).

ms(2)Z5584 point mutation was previously identified as residing in a highly conserved domain of the *rae1* gene. I provided further support that *rae1* is the gene responsible of the observed phenotype in *ms(2)Z5584* mutant, first by RNA interference approach, then by phenotype rescue experiments. Moreover the localization of RAE1 during meiosis and the whole spermatogenesis process was analyzed. The similarities of the cytological phenotypes observed in *rae1* knock-down flies and *ms(2)Z5584* mutants together with the ability of *GFP-rae1* transgene to restore the wild type phenotype in *ms(2)Z5584* homozygous flies, led me to conclude that *rae1* is precisely the gene responsible of the phenotypes observed in *ms(2)Z5584* homozygous mutant males. On the basis of these evidences, future research will be directed toward understanding the RAE1 molecular pathway during the meiotic cell cycle. For this purpose, a molecular approach by Chromatin Immunoprecipitation (ChIP) should lead to RAE1 co-factors identification and, consequently, the molecular pattern in which they are involved. Moreover, a localization analysis of RAE1 in mitotic cells would contribute to a wider characterization of the protein during *Drosophila melanogaster* mitotic cell cycle.

The analysis of cytological defects of *ms(2)Z1168* homozygous mutant males showed anomalies affecting nuclear lamina structure and chromatin condensation process. Due to the absence in bibliography of a description of nuclear lamina behavior during meiotic cell cycle, I performed a complete characterization of nuclear lamina dynamics throughout the wild type spermatogenesis process . Moreover, by genetic and molecular approaches, I identified in the *ms(2)Z1168* strain three mutations affecting a supposed regulatory region of *CG7810* gene. To further support the evidences that the improper *CG7810* expression could be the cause of the mutant phenotype in *ms(2)Z1168,* a gene expression analysis by RT-PCR technique is scheduled to verify the presence of differences in *CG7810* expression between *ms(2)Z1168* homozygous mutant flies and a control wild type strain.

The study of mutant strains in which some steps of spermatogenesis are disrupted allows a broader understanding of the genetic and molecular factors involved in the regulation and in the execution of male meiosis and spermiogenesis.

Due to the high between species conservation in terms of genes and regulatory pathways underlying spermatogenesis, the study of this process in insects represents a powerful tool for the genetic analysis of human spermatogenesis and for future applications to human infertility.

5. MATERIAL AND METHODS

5.1 Fly strains

The *ms(2)Z2-1168* and *ms(2)Z5584* lines were identified by a cytological screen from Zuker collection for EMS-induced male sterile mutations on chromosome 2 and 3 (Wakimoto et al., 2004). The second chromosome lines of Zuker collection carry a mutagenized second chromosome marked with *cn* and *bw* balanced over *CyO, Cy* cn^2. *Oregon-R* line was used for cytological analysis of wild type nuclear lamina behavior. *yw* line was used for fertility test. The following drivers have been used: *BamG4UASDicer* (provided by M. Fuller, Stanford University), *TubG4/TM6: Sb,Tb.* The *UAS-GFP-rae1/TM6B;Sb* stock for RAE1 localization was provided by Chunlai Wu (Neuroscience Center, Louisiana State University). The RNA-interfered lines of *CG7627*, *CG7778, CG7787, CG7810, CG7818, CG7806, CG7795, CG9862* (*rae1*) were obtained from the VDRC. For phenotype rescue experiment the following stock have been used: *w;ST/Sco* (provided by P. Dimitri, University of Rome "Sapienza"), *w; ms(2)Z5584/Sm6a* was generated in the lab. Flies were raised on standard *Drosophila* medium at 25°C. The crosses involving *BamG4UASDicer* line were performed at 29°C.

5.2 Cytological dissection of *rae1* RNA-interfered males

Testes from *rae1* RNA-interfered males were dissected in cold TIB (183mM KCl, 47mM NaCl, 10mM Tris pH 6.8). The slide was frozen in liquid nitrogen and cover slip was removed with a razor blade. Tissues were fixed in cold methanol (-20°C) for 7' and permeabilized in PBT (1X PBS 0.1% Tween20) for 10'. For immunostaining of meiotic spindle and centrosomes testes were incubated in a wet chamber, for 1 hour at room temperature, respectively with the 1: 50 mouse anti-α tubulin monoclonal (Sigma-Aldrich, St. Louis, MO), 1:80 rabbit anti-DSpd2 (kindly provided by S. Bonaccorsi, University of Roma "Sapienza", Giansanti et al., 2008). The primary antibodies were detected by 1 hour incubation at room temperature in a wet and dark chamber with Alexa488-conjugated anti-mouse IgG (Molecular Probes) diluted 1:100 in PBT. Slides were stained in DAPI (2 mg/ml) in 2X SSC for 10' and mounted in vectashield.

5.3 GFP-RAE1 localization during spermatogenesis

Testes from *UASGFPrae;BamG4UASDicer* and *UASGFPrae1/TubG4* (negatively selected for *Sb* marker) males were dissected in cold TIB (183mM KCl, 47mM NaCl, 10mM Tris pH 6.8). The slide was frozen in liquid nitrogen and cover slip was removed with a razor blade. Tissues were fixed in cold methanol (-20°C) for 7' and stained in DAPI (2 mg/ml) in 2X SSC for 10' and mounted in vectashield.

5.4 *ms(2)Z5584* mutant phenotype rescue

Males *ms(2)Z5584* homozygous carrying on the chromosome 3 both *TubG4* and *UASGFPrae1* were obtained according to the crosses outline in figure 8. These males were used for fertility test in a cross with *yw* female and for cytological analysis to verify if the transgene was able to restore the wild type phenotype. The cytology samples were performed as described for GFP-RAE1 localization.

5.5 Cytological dissection of nuclear lamina behavior during spermatogenesis

Testes from *OreR* and *Z2-1168* very young adult males (up to two day-old), were dissected in cold TIB (183mM KCl, 47mM NaCl, 10mM Tris pH 6.8). Testes were transferred in a drop (10 μl) of TIB solution on a slide and, once put on a siliconized cover slip, the slide was frozen in liquid nitrogen and cover slip was removed with a razor blade. Tissues were fixed in cold methanol (-20°C) for 7' and permeabilized in PBT (1X PBS 0.1% Tween20) for 10'. For immunostaining of nuclear lamina, testes were incubated in a wet chamber, for 1 hour at room temperature, with the monoclonal mouse anti-laminDm0 IgG (Developmental Studies Hybridoma Bank –DSHB- Department of Biological Sciences, University of Iowa) diluted 1:50 in PBT. The primary antibodies were detected by 1 hour incubation at room temperature in a wet and dark chamber with Alexa488-conjugated anti-mouse IgG (Molecular Probes) diluted 1:100 in PBT. Slides were stained in DAPI (2 mg/ml) in 2X SSC for 10' and mounted in vectashield.

5.6 Confocal microscopy

Samples were examined using a Zeiss LSM-710 confocal microscope equipped with digital microscope camera AxioCam; images were captured by Zeiss Plan-Apochromat 63x/1.40 Oil DIC M27 objective, using standard software ZEN. Images were processed using Adobe Photoshop.

5.7 *In vivo* cytology of RNA-interfered males for gene identification in *ms(2)Z1168* mutant

Live testes of young males (less than two day-old) were dissected in TIB (183 mM KCl, 47 mM NaCl, 10 mM Tris pH 6.8), transferred in another drop (10 μ l) of TIB on a slide, squashed and examined by phase contrast microscopy.

5.8 *CG7810* Sequencing

Genomic DNA from males and females of *ms(2)Z1168/ ms(2)Z1168* and *ms(2)Z5584/ ms(2)Z5584* flies were extracted by standard phenol-chloroform extraction method. A combination of primers were designed (see below) to amplify the whole CG7810 gene region and used in an enzymatic amplification reactions with the following program: 95°C for 3', 94°C per 30" than 30” at Tm and 30” at 72°C repeated 30 times. Finally, 72°C per 10". The PCR products were purified with Wizard SV Gel and PCR Clean-Up System Kit (Promega), sequenced and compared with wild type *CG7810* sequence from NCBI database and with *CG7810* sequence from *ms(2)Z5584/ ms(2)Z5584* strain.

***CG7810* sequence and primers used for PCR amplification**

GTCGCCCCAGTCCACCACAGATGACATCTCGATCGAAATCTTTGATGGAT
TCTTTGGTCTTCCGCTAAACTTGCTCAGTTAGTCATCGCTGCCTGCATAT
TTGCACCACTGAACCACCGAGTGGCGTTAAACAAAGCGATAAACACAACA
ATTGGACCTCAGATAAAGTTCGTAATGAAAATACAGCCGCTATGTGGAGC
→→→→→→→→→→→→→→→→→→→→
CGCAGGGTTGCCAACTATCAAAATCGTTGAACGGTTTCCTTTTCGTCTTT
TTTTTTGAATGGAAATATTTTCATTGTATTATGCATAATACATATTTTCA
AAGATCGTAATTTTTTTTTTCAGACAGAGAACTTGGTTTATTTTCACAATC
GCTAATTTTTTATCGAAAAATTTAATTACTCTGGCAACTCTATGTAAATG
ACATTGGCTAAGAAAGAAGAAGCATTTGTTTACGTTTCTATTTCACACTT
TGTGCAATTTGTGTAAACAATTATGACAACTGGAAGCGATGCTGACGGGG
ATGGTGACCACCAGGGCAACAATGACATCGTCCCAAATCCAGAACATCCT
→→→→→→→→→→→→→→→→→→→→
CCGGAGATAATAGACATCTTCAAATCCTTGGCCGAAAACAATCAAATCGT
CTTTAAGTCGCAGCAAATTGATGATCCGGAAATTCCGGTCGAAGAGAAGC
←←←←←←←←←←←←←←←←←←←←
AACAAATAGCACGAGATGCCTTCGATAAGAACCGTGAGAACTTTCTCATC
←←←
CGATTTGGAGGCTTCCTGAATGTAAGACAACTGGGTTCCTTCCAGGAACT
GGCTGTCAAGGAACCCATTAAAGCAGATGAAAATCTGGAGGAGATGTGCC
TGCTGCTAGAGGATTTTAGGAGGAAACTCAACACTCGTGCGGTATCCATT
AAAAACCGAAGATACCATGCCATGCAGCAGCTCCTTGACAAGGGAGAATA
CTTTAGCGAACACGAGATGATGCAAAGGGCGCCGGATCTCTACCAGGAGC
TAGTGGGTCAGTACCTAACGGAGGCGGAAAAGAAGGCTCGGGATAGTTAC
→→→→→→→→→→→→→→→→→→→→
GATGTTCGGAATACTAGCTTCTCAGGAATACTAATGCATACGTTGGAGAA
AAAGCAAAGAGATGAATTACTAGAGGAAACGCAGCAGGAAGGAAAGCAGA
←←←←←←←←←←←←←←←←←←←←
GCGTGCAGGTCACAAGTGAATCCAATCCTCAGGCAGACTGTGACGTTCCT
GTCGCTTGCCGAAAGCAGTGGGGTGGATTTGAAGATGATGAACCAGTGGC
CTGTTCAACGAGTCGAAATGCGGAAGTCCGAGCTCCAATGAATACAACTA
→→→→→→→→→→→→→→→→→→→→
TGATCTCCACACCGGAGTTCTATAATCCTGGAGAGCGAGAACTACTACGC
AATGAGTTCTTGAGTATGATGAAGGAACGCTTTCTTAGTGGCGAAGACAA
GGATTTTGATTATAAGGCCGTAGATGATAACACTTTGCTGGATGATCTGA
AGCAAATTGAGCAGGATGAAGAAGATGCCTACTTTGAGGATAGCGAGGAC
←←←←←←←←←←←←←←←←←←←←
GAGGAGGAATTGGAGGAGCATGCTGCGGATGAGAATGCTATATCTAGCGA
←←←←←←←←←←←←←←←←←←←←
AGATGACTTGGATATCTACATGAGGCATCTAAGCAATCATCACAGTCTCC
AGAATAGTCACGGATAATAAATGAAAGCTGCTGGTCGCTCGGCATCCAAA
GAAAACCCTGGAAATCGATAGGATACTCAGCATTCTGCAGCAATAGACTT
TAATGTTAATCTTATTCTTAGCCTTAAAAACTTTTGATCTTAGACACTAG
AATACACGCAGTTGTTGAGTAAAAATGCTGTTATCTGGGCCTTCCACGAC
CACGTGGAAAGCCGCGTCCTCTTCCTCTTAAAACTTTGCTATTCGGCGGC
GGACTCTTGGGCCTCAGTAGTTCAATCCTACTAGTGCAACCGGTGGCTGG
AGCCTCAGCAAAGTAGGTCTGGTATAGCTCGGAGTTGAAGTTCGAGTTCG
TCAGTTCCGGACCAACAGTTAGCCAACCTGGTCGAATACTCGAATCTCTG
CCGAACAGATGCAAACGCCGTCGACCCAAGCAGAAATGTTCGATGATGTG
AAAGATCTCGATGGGCTTCTCGAAGCTGCCAAACTCCTCTTCCTCTGAGA
TGATTAAATCAATGTCCACGTTGGCATGGATAAAATCGCCATCAGTGGAG
CGGCGAACAGTTCCTTTGATTCCCATCAGGCAGTGTTCCTTGGTGCGTTG
←←←←←←←←←←←←←←←←←←←←
AAAGACCGCTTTCGGTTCAAGTTGCTTGGAGTGCCCGGGCTTGTTAATGT
←←←←←←←←←←←←←←←←←←←←
TGGTCCGTATCCAACATATGTCTTCGCACCTCCGGAATCCCCACTTCTTC

XXXX Forward Primer **XXXX Reverse Primer**

6. REFERENCES

Alphey L., Jimenez J., White-Cooper H., Dawson L., Nurse P., Glover D.M. (1992). *Twine*, a cdc25 homolog that functions in the male and female germline of *Drosophila*. *Cell* 69: 977-988.

Alsheimer M., Benavente R. (1996). Change of karyoskeleton during mammalian spermatogenesis: expression pattern of nuclear lamin C2 and its regulation. *Exp. Cell. Res.* 228(2):181-8.

Alsheimer M., Fecher E., Benavente R. (1998). Nuclear envelope remodelling during rat spermiogenesis: distribution and expression pattern of LAP2/thymopoietins. *J. Cell. Sci.* 111:2227-34.

Alsheimer, M., von Glasenapp, E., Hock, R., and Benavente, R. (1999). Architecture of the nuclear periphery of rat pachytene spermatocytes: Distribution of nuclear envelope proteins in relation to synaptonemal complex attachment sites. *Mol. Biol. Cell.* 10: 1235–1245.

Arkhipova, I.R. (1995). Promoter elements in *Drosophila melanogaster* revealed by sequence analysis. *Genetics* 139(3):1359-69.

Ayyar S., Jiang J., Collu A., White-Cooper H. & White R. (2003). Drosophila TGIF is essential for developmentally regulated transcription in spermatogenesis. *Development* 130: 2841–2852.

Babu, J. R., Jeganathan, K. B., Baker, D. J., Wu, X., Kang-Decker, N. and van Deursen, J. M. (2003). Rae1 is an essential mitotic checkpoint regulator that cooperates with Bub3 to prevent chromosome missegregation. *J. Cell Biol.* 160: 341-353.

Barreau C., Benson E., White-Cooper H. (2008). *Comet* and *cup* genes in Drosophila spermatogenesis: the first demonstration of post-meiotic transcription. *Biochemical Society Transactions* 36: 504-2.

Basu, J., Bousbaa, H., Logarinho, E., Li, Z., Williams, B. C., Lopes, C., Sunkel, C. E. and Goldberg, M. L. (1999). Mutations in the essential spindle checkpoint gene *bub1* cause chromosome missegregation and fail to block apoptosis in Drosophila. *J. Cell Biol.* 146: 13-28.

Beall E.L., Lewis P.W., Bell M., Rocha M., Jones D.L. & Botchan M. (2007). Discovery of tMAC: a Drosophila testis-specific meiotic arrest complex paralogous to Myb-MuvB. *Genes and Development* 21: 904–919.

Beaudouin J., Gerlich D., Daigle N., Eils R., Ellenberg J. (2002). Nuclear envelope breakdown proceeds by microtubule-induced tearing of the lamina. *Cell* 108, 83–96.

Bergner LM, Hickman FE, Wood KH, Wakeman CM, Stone HH, Campbell TJ, Lightcap SB, Favors SM, Aldridge AC, Hales KG. (2010). A novel predicted bromodomain-related protein affects coordination between meiosis and spermiogenesis in Drosophila and is required for male meiotic cytokinesis. *DNA Cell Biol*. 29(9):487-98.

Bharathi, A., Ghosh, A., Whalen, W. A., Yoon, J. H., Pu, R., Dasso, M. and Dhar, R. (1997). The human RAE1 gene is a functional homologue of *Schizosaccharomyces pombe rae1* gene involved in nuclear export of Poly(A)$^+$ RNA. *Gene* 198: 251-258.

Blower, M. D., Nachury, M., Heald, R. and Weis, K. (2005). A Rae1-containing ribonucleoprotein complex is required for mitotic spindle assembly. *Cell* 121: 223-234.

Bowen, R. H. (1922). Studies on insect spermatogenesis. III. On the structure of the nebenkern in the insect spermatid and the origin of the nebenkern patterns. *Biol. Bull.* 42: 53-85.

Brown, J. A., Bharathi, A., Ghosh, A., Whalen, W., Fitzgerald, E .and Dhar, R. (1995). A mutation in the *Schizosaccharomyces pombe rae1* gene causes defects in Poly(A)$^+$ RNA export and in the cytoskeleton. *J. Biol. Chem.* 270: 7411-7419.

Cenci G., Bonaccorsi S., Pisano C., Verni F., Gatti M. (1994). Chromatin and microtubule organization during premeiotic, meiotic and early postmeiotic stages of *Drosophila melanogaster* spermatogenesis. *Journal of Cell Science* 107: 3521-3534

Chen X., Hiller M.A., Sancak Y. and Fuller M.T. (2005). Tissue-specific TAFs counteract Polycomb to turn on terminal differentiation. *Science* 310: 869–872.

Courtot C., Fankhauser C., Simanis V., Lehner C.F. (1992). The *Drosophila cdc25* homolog *twine* is required for meiosis. *Development* 116: 405-416.

D'Angelo MA, Hetzer MW. (2006). The role of the nuclear envelope in cellular organization. *Cell Mol Life Sci*. 63(3):316-32.

Dechat T., Adam S.A., Taimen P., Shimi T., Goldman RD. (2010). Nuclear lamins. *Cold Spring Harb Perspect Biol*. 2(11):a000547.

Dechat T., Pfleghaar K., Sengupta K., Shimi T., Shumaker D.K., Solimando L., Goldman R.D. (2008). Nuclear lamins: major factors in the structural organization and function of the nucleus and chromatin. *Genes Dev*. 22(7):832-53.

Dunphy W.G. and Kumagai A. (1991). The cdc25 protein contains an intrinsic phosphatase activity. *Cell* 67(1): 189-96.

Eberhart C.G., Maines J.Z., Wasserman S.A. (1996). Meiotic cell cycle requirement for a fly homologue of human *Deleted in Azoospermia. Nature* 381: 783-785.

Eberhart C.G., Wasserman S.A. (1995). The pelota locus encodes a protein required for meiotic cell division: an analysis of G2/M arrest in *Drosophila* spermatogenesis. *Development* 121: 3477-86.

Edgar B.A. and O'Farrell P.H. (1989). Genetic control of cell division patterns in the Drosophila embryo. *Cell* 57: 177-87.

Fabrizio J., Hime G., Lemmon S.K., Bazinet C. (1998). Genetic dissection of sperm individualization in *Drosophila melanogaster. Development* 125: 1833-1843.

Fawcett DW. (1966). On the occurrence of a fibrous lamina on the inner aspect of the nuclear envelope in certain cells of vertebrates. *Am. J. Anat.* 119: 129–145.

Fisher D.Z., Chaudhary N., and Blobel G. (1986). cDNA sequencing of nuclear lamins A and C reveals primary and secondary structural homology to intermediate filament proteins. *Proc. Natl. Acad. Sci.* 83: 6450–6454.

Foisner R1, Gerace L. (1993). Integral membrane proteins of the nuclear envelope interact with lamins and chromosomes, and binding is modulated by mitotic phosphorylation. *Cel*l 73(7):1267-79.

Fuchs, J. P., Giloh, H., Kuo, C. H., Saumweber, H. and Sedat, J. W. (1983). Nuclear structure: Determination of the fate of the nuclear envelope in *Drosophila* during mitosis using monoclonal antibodies. *J. Cell Sci.* 64: 331-349.

Fuller, M.T. (1993). Spermatogenesis. In The Development of *Drosophila melanogaster*. *Cold Spring Harbor Laboratory Press* Vol. 1: 71-147.

Fuller M.T. (1998). Genetic control of cell proliferation and differentiation in Drosophila spermatogenesis. *Semin Cell Dev Biol*. 9(4): 379-391.

Furukawa K., and Hotta Y. (1993). cDNA cloning of a germ cell specific lamin B3 from mouse spermatocytes and analysis of its function by ectopic expression in somatic cells. *EMBO J.*12: 97–106.

Furukawa K., Inagaki H., and Hotta Y. (1994). Identification and cloning of an mRNA coding for a germ cell-specific A- type lamin in mice. *Exp. Cell Res.* 212: 426–430.

Gautier J, Solomon MJ, Booher RN, Bazan JF, Kirschner MW. (1991). cdc25 is a specific tyrosine phosphatase that directly activates p34cdc2. *Cell*. 4;67(1):197-211.

Georgatos SD, Pyrpasopoulou A, Theodoropoulos PA. (1997). Nuclear envelope breakdown in mammalian cells involves stepwise lamina disassembly and microtubule-drive deformation of the nuclear membrane. *J. Cell Sci*. 110:2129-4.

Gerace L, Blobel G. (1980). The nuclear envelope lamina is reversibly depolymerized during mitosis. *Cell.* 19(1):277-87.

Gerace, L., Blum, A. and BlobelA, G. (1978). Immunoctyochemical localization of the major polypeptides of the nuclear pore complex—lamina fraction. *Cell Biol.* 79: 546-566.

Glotzer M, Murray AW, Kirschner MW. (1991). Cyclin is degraded by the ubiquitin pathway. *Nature* 349(6305):132-8.

Gould K.L., Moreno S., Tonks N.K., Nurse P. (1990). Complementation of the mitotic activator, p80cdc25, by a human protein-tyrosine phosphatase. *Science* 14, 250(4987):1573-6.

Gönczy P, Thomas BJ, DiNardo S. (1994). *roughex* is a dose-dependent regulator of the second meiotic division during Drosophila spermatogenesis. *Cell.* 77(7):1015-25.

Grill B, Chen L, Tulgren ED, Baker ST, Bienvenut W, Anderson M, Quadroni M, Jin Y, Garner CC. (2012). RAE-1, a novel PHR binding protein, is required for axon termination and synapse formation in *Caenorhabditis elegans*. *J. Neurosci*. 32(8):2628-36.

Gruenbaum Y. (2000). Essential roles for *Caenorhabditis elegans* lamin gene in nuclear organization, cell cycle progression, and spatial organization of nuclear pore complexes. *Mol. Biol. Cell*. 11(11):3937-47.

Harel A, Zlotkin E, Nainudel-Epszteyn S, Feinstein N, Fisher PA, Gruenbaum Y. (1989). Persistence of major nuclear envelope antigens in an envelope-like structure during mitosis in *Drosophila melanogaster* embryos. *J. Cell Sci*. 94:463-70.

Hiller M.A., Chen X., Pringle M.J., Suchorolski M., Sancak Y., Viswanathan S., Bolival B., Lin T-Y, Marino S. & Fuller M.T. (2004). Testis-specific TAF homologs collaborate to control a tissue-specific transcription program. *Development* 131: 5297-5308.

Hiller MA, Lin TY, Wood C, Fuller MT. (2001). Developmental regulation of transcription by a tissue-specific TAF homolog. *Genes Dev.* 15;15(8):1021-30.

Hiraoka Y, Agard DA, Sedat JW. (1990). Temporal and spatial coordination of chromosome movement, spindle formation, and nuclear envelope breakdown during prometaphase in *Drosophila melanogaster* embryos. *J. Cell Biol*. 111:2815-28.

Jayaramaiah R. S, Renkawitz-Pohl R. (2005). Replacement by *Drosophila melanogaster* protamines and Mst77F of histones during chromatin condensation in late spermatids and role of sesame in the removal of these proteins from the male pronucleus. *Mol. Cell Biol*. 25(14):6165-77.

Jeganathan, K. B, Baker, D. J., van Deursen, J.M. (2006). Securin associates with APCCdh1 in prometaphase but its destruction is delayed by Rae1 and Nup98 until the metaphase/anaphase transition. *Cell Cycle* 5: 366-370.

Jiang J., Benson E., Bausek N., Doggett K. &White-Cooper H. (2007). Tombola, a tesmin/TSO1 family protein, regulates transcriptional activation in the Drosophila male germline and physically interacts with *always early*. *Development* 134: 1549-1559.

Jiang J. and White-Cooper H. (2003). Transcriptional activation in *Drosophila* spermatogenesis involves the mutually dependent function of *aly* and a novel meiotic arrest gene *cookie monster*. *Development* 130: 563-573.

Jimenez J., Alphey L., Nurse P., Glover D.M. (1990). Complementation of fission yeast cdc2ts and cdc25ts mutants identifies two cell cycle genes from Drosophila: a *cdc2* homologue and *string*. *EMBO J*. 9: 3565-71.

Kiger A. A., Jones D. L., Schulz C., Rogers M. B., Fuller M. T. (2001). Stem cell self-renewal specified by JAK-STAT activation in response to a support cell cue. *Science* 294: 2542-2545.

Kimura T., C. Ito, S.Watanabe, T. Takahashi, M. Ikawa, K. Yomogida, Y. Fujita, M. Ikeuchi, N. Asada, K. Matsumiya, A. Okuyama, M. Okabe, K. Toshimori, T. Nakano. (2003). Mouse germ cell-less as an essential component of nuclear integrity. *Mol. Cell. Biol*. 23: 1304-1315.

Krek W. and Nigg E.A. (1991). Mutations of p34cdc2 phosphorylation sites induce premature mitotic events in HeLa cells: evidence for a double block to p34cdc2 kinase activation in vertebrates. *EMBO J.* 10(11): 3331-41.

Lee JJ, von Kessler DP, Parks S, Beachy PA. (1992). Secretion and localized transcription suggest a role in positional signaling for products of the segmentation gene *hedgehog*. *Cell*. 71(1):33-50.

Lenz-Böhme B., Wismar J., Fuchs S., Reifegerste R., Buchner E., Betz H., Schmitt B. (1997). Insertional mutation of the Drosophila nuclear *lamin Dm0* gene results in defective nuclear envelopes, clustering of nuclear pore complexes, and accumulation of annulate lamellae. *J Cell Biol*. 137(5):1001-16.

Lewis P.W., Beall E.L., Fleischer T.C., Georlette D., Link A.J. & Botchan M. (2004). Identification of a Drosophila Myb-E2F2/RBF transcriptional repressor complex. *Genes and Development* 18: 2929-2940.

Lindsley D. and Tokuyasu K.T. (1980). Spermatogenesis, in genetics and biology of Drosophila. *Academic Press* Vol. 2: 225-294.

Liu J, Rolef Ben-Shahar T, Riemer D, Treinin M, Spann P, Weber K, Fire A,

Gruenbaum Y. (2000). Essential roles for *Caenorhabditis elegans* lamin gene in nuclear organization, cell cycle progression, and spatial organization of nuclear pore complexes. *Mol Biol Cell*. 11(11):3937-47.

Luderus M.E, **de Graaf A, Mattia E, den Blaauwen JL, Grande MA, de Jong L, van Driel R.** (1992). Binding of matrix attachment regions to lamin B1. *Cell* 70: 949-959.

Machiels B.M., Zorenc A.H., Endert J.M., Kuijpers H.J., van Eys G.J., Ramaekers F.C., and Broers J.L. (1996). An alternative splicing product of the lamin A/C gene lacks exon 10. *J. Biol. Chem.* 271: 9249–9253.

Maines J. and Wasserman S. (1998). Regulation and execution of meiosis in Drosophila males. *Curr. Top. Dev. Biol*. 37: 301-332.

Mathog D. and Sedat J.W. (1989). The three-dimensional organization of polytene nuclei in Drosophila melanogaster with compound Xy or ring X chromosomes. *Genetics* 121: 293-311.

McKeon F.D., Kirschner M.W., and Caput D. (1986). Homologies in both primary and secondary structure between nuclear envelope and intermediate filament proteins. *Nature* 319: 463–468.

Moir, R. D., Montag-Lowy, M., and Goldman, R. D. (1994). Dynamic properties of nuclear lamins: Lamin B is associated with sites of DNAreplication. *J. Cell Biol.* 125: 1201–1212.

Moir R.D., Spann T.P., Herrmann H., and Goldman R.D. (2000). Disruption of nuclear lamin organization blocks the elongation phase of DNA replication. *J. Cell Biol.* 149: 1179-1192.

Murphy, R., Watkins, J. L., Wente, S. R. (1996). GLE2, a *Saccharomyces cerevisiae* homologue of the *Schizosaccharomyces pombe* export factor RAE1, is required for nuclear pore complex structure and function. *Mol. Biol. Cell* 7: 1921-1937.

Mylonis I., Drosou V., Brancorsini S., Nikolakaki E., Sassone- Corsi P., Ginnakouros T. (2004). Temporal association of protamine 1 with the inner nuclear membrane protein lamin B receptor during spermiogenesis. *J. Biol. Chem.* 279: 11626–11631.

Nakano, H., Funasaka, T., Hashizume, C., Wong, R. W. (2010). Nucleoporin translocated promoter region (Tpr) associates with dynein complex, preventing chromosome lagging formation during mitosis. *J. Biol. Chem.* 285: 10841-10849.

Neer, E.J., Schmidt, C. J., Nambudripad, R., Smith, T. F. (1994). The ancient regulatory-protein family of WD-repeat proteins. *Nature* 371: 297-300.

Newport, J. W., Wilson, K. L., and Dunphy, W. G. (1990). A lamin-independent pathway for nuclear envelope assembly. *J.Cell Biol.* 111: 2247–2259.

Norbury C., Blow J., Nurse P. (1991). Regulatory phosphorylation of the p34cdc2 protein kinase in vertebrates. *EMBO J.* 10(11): 3321-9.

Nurse P. (1990). Universal control mechanism regulating onset of M-phase. *Nature* 344: 503-8.

Paddy, M. R., Belmont, A. S., Saumweber, H., Agard, D. A., and Sedat, J. W. (1990). Interphase nuclear envelope lamins form a discontinuous network that interacts with only a fraction of the chromatin in the nuclear periphery. *Cell* 62: 89-106.

Paddy MR, Saumweber H, Agard DA, Sedat JW. (1996). Time-resolved, in vivo studies of mitotic spindle formation and nuclear lamina breakdown in Drosophila early embryos. *J. Cell Sci.* 109:591-607.

Peifer M, McCrea PD, Green KJ, Wieschaus E, Gumbiner BMJ Cell Biol. (1992). The vertebrate adhesive junction proteins beta-catenin and plakoglobin and the Drosophila segment polarity gene armadillo form a multigene family with similar properties. *J. Cell Biol.* 118(3):681-91.

Perezgazga L., Jiang J., Bolival B., Hiller M., Benson E., Fuller M.T. & White-Cooper H. (2004). Regulation of transcription of meiotic cell cycle and terminal differentiation genes by the testis-specific Zn finger protein matotopetli. *Development* 131: 1691-1702.

Pollard K.M., Chan E.K., Grant B.J., Sullivan K.F., Tan E.M., and Glass C.A. (1990). In vitro posttranslational modification of lamin B cloned from a human T-cell line. *Mol. Cell. Biol.*10: 2164–2175.

Pritchard, C. E., Fornerod, M., Kasper, L. H., Van Deursen, J. M. (1999). RAE1 is a shuttling mRNA export factor that binds to a GLEBS-like NUP98 motif at the nuclear pore complex through multiple domains. *J. Cell Biol.* 145: 237-253.

Rathke C., Barrends W. M., Jayaramaiah Raja S., Bartkuhn M., Renkawitz R., Renkawitz-Pohl R. (2007). Transition from a nucleosome-based to a protamin-based chromatin configuration during spermiogenesis in *Drosophila*. *J. Cell Sci.* 120: 1689-1700.

Reddy K.L., Zullo J.M., Bertolino E., and Singh H. (2008). Transcriptional repression mediated by repositioning of genes to the nuclear lamina. *Nature 452*: 243-247.

Rober R.A., Weber K., and Osborn M. (1989). Differential timing of nuclear lamin A/C expression in the various organs of the mouse embryo and the young animal: A developmental study. *Development* 105: 365–378.

Schütz W., Alsheimer M., Ollinger R., Benavente R. (2005). Nuclear envelope remodeling during mouse spermiogenesis: postmeiotic expression and redistribution of germline lamin B3. *Exp Cell Res.* 307(2): 285-91.

Shumaker D.K., Solimando L., Sengupta K., Shimi T., Adam S.A., Grunwald A., Strelkov S.V., Aebi U., Cardoso M.C., Goldman R.D. (2008). The highly conserved

nuclear lamin Ig-fold binds to PCNA: its role in DNA replication. *J. Cell Biol.* 181(2): 269-80.

Sitterlin, D. (2004). Characterization of the *Drosophila* Rae1 protein as a G1 phase regulator of the cell cycle. *Gene* 326: 107-116.

Smith TF. (2008). Diversity of WD-repeat proteins. *Subcell Biochem*. 48:20-30.

Smith D.E., Fisher P.A. (1989). Interconversion of Drosophila nuclear lamin isoforms during oogenesis, early embryogenesis, and upon entry of cultured cells into mitosis. *J Cell Biol.* 108(2):255-65.

Smith D.E., Gruenbaum Y., Berrios M., Fisher P.A. (1987). Biosynthesis and interconversion of Drosophila nuclear lamin isoforms during normal growth and in response to heat shock. *J. Cell Biol.* 105: 771–790.

Stern B., Ried G., Clegg N.J., Grigliatti T.A., Lehner C.F. (1993). Genetic analysis of the Drosophila *cdc2* homolog. *Development* 117: 219-32.

Strausfeld U, Labbé JC, Fesquet D, Cavadore JC, Picard A, Sadhu K, Russell P, Dorée M. (1991). Dephosphorylation and activation of a p34cdc2/cyclin B complex in vitro by human CDC25 protein. *Nature* 16;351(6323):242-5.

Taniura, H., Glass, C., and Gerace, L. (1995). A chromatin binding site in the tail domain of nuclear lamins that interacts with core histones. *J. Cell Biol.* 131, 33-44.

Tates, A. D. (1971). Cytodifferentiation during spermatogenesis in *Drosophila melanogaster*: an electron microscope study. Ph.D. thesis. Rijksuniversiteit, Leiden. (Tates thesis has been extensively reviewed by Fuller, 1993).

Tian, X., Li, J., Valakh, V., DiAntonio, A., Wu, C. (2011). *Drosophila* Rae1 controls the abundance of the ubiquitin ligase Highwire in post-mitotic neurons. *Nature Neuroscience* 14: 1267-1277.

Tokuyasu K.T. (1975). Dynamics of spermiogenesis in *Drosophila melanogaster*. VI. Significance of "onion" nebenkern formation. *J. Ultrastruct. Res.* 53: 93-112.

Tulina N. and Matunis E. (2001). Control of stem cell self-renewal in Drosophila spermatogenesis by JAK-STAT signalling. *Science* 294: 2546-2549.

Vester B., Smith A., Krohne G., Benavente R. (1993). Presence of a nuclear lamina in pachytene spermatocytes of the rat. *J. Cell Sci*. 104: 557-563.

Volpi S., Bongiorni S., Fabbretti F., Wakimoto B.T., Prantera G. (2013). Drosophila *rae1* is required for male meiosis and spermatogenesis. *J. Cell S.* 126: 3541-51.

Wakimoto B.T., Lindsley D.L., Herrera C. (2004). Toward a comprehensive genetic analysis of male fertility in *Drosophila melanogaster*. *Genetics* 167: 207-16.

Wan HI, DiAntonio A, Fetter RD, Bergstrom K, Strauss R, Goodman CS. (2000). *Highwire* regulates synaptic growth in Drosophila. *Neuron.* 26(2):313-29.

Wang, X., Babu, J. R., Harden, J. M., Jablonski, S. A., Gazi, M. H., Lingle, W. L., de Groen, P. C., Yen, T. J., van Deursen, J. M. (2001). The mitotic checkpoint protein hBUB3 and the mRNA export factor hRAE1 interact with GLE2p-binding sequence (GLEBS)-containing proteins. *J. Biol. Chem.* 276: 26559-26567.

Wang Z. and Mann R.S. (2003). Requirement for two nearly identical TGIF-related homeobox genes in Drosophila spermatogensis. *Development* 130: 2853-2865.

Whalen, W. A, Bharathi, A., Danielewicz, D., Dhar, R. (1997). Advancement through mitosis requires *rae1* gene function in fission yeast. *Yeast* 13: 1167-1179.

White-Cooper H. (2012)**.** Tissue, cell type and stage-specific ectopic gene expression and RNAi induction in the Drosophila testis. *Landes Bioscience*.

White-Cooper H. (2010). Molecular mechanism of gene regulation during Drosophila

spermatogenesis. *Reproduction* 139: 11-12.

White-Cooper H., Alphey L., Glover D.M. (1993). The *cdc25* homologue *twine* is required for only some aspects of the entry into meiosis in *Drosophila*. *J. Cell S.* 106: 1035-1044.

White-Cooper H., Leroy D., MacQueen A.,Fuller M.T. (2000). Transcription of meiotic cell cycle and terminal differentiation genes depends on a conserved chromatin associated protein, whose nuclear localisation is regulated. *Development* 127: 5463–5473.

White-Cooper H., Schafer M.A., Alphey L.S., Fuller M.T. (1998). Transcriptional and post-transcriptional control mechanisms coordinate the onset of spermatid differentiation with meiosis I in Drosophila. *Development* 125: 125-134.

Wong, R. W., Blobel, G., Coutavas, E. (2006). Rae1 interaction with NuMA is required for bipolar spindle formation. *Proc Natl Acad Sci USA* **1**03: 19783-19787.